The Journal of Supercritical Fluids 202 (2023) 106058

Contents lists available at ScienceDirect

The Journal of Supercritical Fluids

journal homepage: www.elsevier.com/locate/supflu

The transformation of cellulose acetate into a new biocidal polymer by effluent-free grafting in supercritical carbon dioxide

Mariusz Nowak [a], Damian Semba [a], Dusan Misic [b], Tomasz Półbrat [b], Dusica Stojanovic [c], Slavoljub Stanojevic [d], Anna Trusek [a], Irena Zizovic [a,*]

[a] Faculty of Chemistry, Wroclaw University of Science and Technology, Wybrzeze Wyspianskiego 27, Wroclaw, 50–370, Poland
[b] Faculty of Biotechnology and Food Science, Wroclaw University of Environmental and Life Sciences, Wroclaw, 51–651, Poland
[c] Faculty of Technology and Metallurgy, University of Belgrade, Karnegijeva 4, 11 000 Belgrade, Serbia
[d] Ministry of Agriculture, Forestry and Water Management, Directorate for National Reference Laboratories, 11080 Zemun, Serbia

HIGHLIGHTS

- New biocidal polymer with strong anti-adhesion activity was developed.
- An effluent-free route for cellulose acetate grafting was presented.
- Grafting occurred in the whole polymer volume providing hydrophobic properties.
- *S. aureus* (incl. MRSA), *E. coli*, and *S.* Enteritidis could not attach to the polymer.
- Microbiological vs. statistical significance was discussed with scientific arguments.

GRAPHICAL ABSTRACT

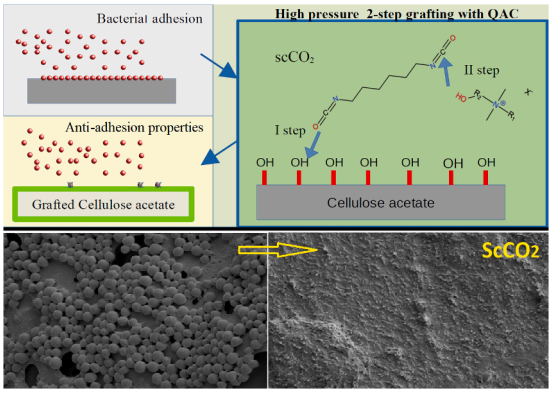

ARTICLE INFO

Keywords:
Biocidal polymer
Cellulose acetate
Quaternary ammonium compounds
Antibiofilm
Supercritical carbon dioxide
MRSA

ABSTRACT

The study reports an effluent-free, green process for the production of materials with favorable antibiofilm properties by cellulose acetate grafting with quaternary ammonium compounds in supercritical carbon dioxide. Two quaternary ammonium compounds, N-(2-Hydroxyethyl)-N,N-dimethylundecan-1-aminium Bromide and N-(11-Hydroxyundecanyl-N,N-dimethyltetradecan- 1-aminium Bromide, were synthesized and chemically attached to cellulose acetate via hexamethylene diisocyanate as a linker under the conditions of 30 MPa and 70 °C. The polymer modification occurred in its whole volume. The chemical conversion led to a decrease in the degree of crystallinity and the appearance of a rugged polymer surface. However, the cross-section imaging of the newly obtained materials revealed a compact polymer structure. The functionalized materials acquired hydrophobic properties. Microbiological tests showed the impossibility of *Staphylococcus aureus* ATCC 29213, Methicillin-resistant *Staphylococcus aureus* ATCC 43300, *Escherichia coli* ATCC 10536, and *Salmonella* Enteritidis ATCC 13076 attachment to the material obtained by the cellulose acetate grafting procedure with N-(11-Hydroxyundecanyl-N,N-dimethyltetradecan- 1-aminium Bromide.

* Corresponding author.
E-mail address: irena.zizovic@pwr.edu.pl (I. Zizovic).

https://doi.org/10.1016/j.supflu.2023.106058
Received 2 July 2023; Received in revised form 12 August 2023; Accepted 15 August 2023
Available online 16 August 2023

1. Introduction

The chemical integration of biocides, *e.g.*, quaternary ammonium compounds (QACs), into the polymer structure results in forming a so-called biocidal polymer [1]. Biocidal polymers do not release the active substance into the environment, and their antimicrobial activity is based mainly on contact inhibition. The most significant advantage of such modifications is the prolonged duration of the antibacterial activity [1].

Biofilms are multicellular structures formed after the adhesion of bacteria to surfaces and their synchronized multiplication and excretion of the so-called extracellular (polymeric) matrix in which they stay protected from unfavorable environmental conditions, disinfectants, antibiotics, UV radiation, drying, and high temperatures [2–4]. Biofilm formation presents a significant problem in hospitals, water treatment units, bioreactors, and the food industry. Most pathogenic bacteria, including foodborne pathogens, are capable of forming biofilms on abiotic surfaces made of plastic, stainless steel, wood, and glass [2–4]. Medical devices such as orthopedic, dental and tissue implants, contact lenses, surgical sutures, prosthetic joints, catheters, and heart valves, are materials to which pathogenic bacteria have the ability to adhere and produce strong biofilms [5,6]. Therefore, the term "medical-device associated infections" (MDAI) was introduced, and it essentially represents a medical complication caused by pathogenic bacteria from biofilms formed on the surface of implanted medical polymers [5,6]. It is unanimously considered that bacteria's successful adhesion to the surface is the first and basic prerequisite for forming biofilms [7]. Thus, the most promising strategy against biofilms is the technology of production and design of new polymeric materials on which the formation of biofilms would be impossible [5,8].

Cellulose acetate (CA) is obtained by the acetylation of cellulose, the most abundant natural polymer. It is considered a renewable and biodegradable polymer, used to make a variety of products, including textiles, plastics, films, membranes in liquid and gas separations, and many others, thus being incorporated in almost all pores of modern life [9]. CA and its composites have also been readily applied for medical purposes because CA meets many biomedical implant requirements [10]. Outstanding biocompatibility, biodegradability, non-toxicity, excellent tissue integration, and immunological neutrality of CA are the most important features for the medical use of this relatively inexpensive and easily accessible material [11]. CA is used in tissue and cell culture engineering, immobilization and delivery of bioactive substances, wound healing, and biosensor design [12–14].

The advantageous properties of supercritical fluids allow for the production of novel and unique materials that can't be obtained otherwise [15–18]. Carbon dioxide is the most used supercritical fluid for polymer processing due to its favorable critical temperature and high solubility in polymers [19]. The application of $scCO_2$ in impregnation and grafting purposes attracts considerable attention nowadays because of the complete effluent elimination in the process, thus avoiding the problem of handling and disposal of vast amounts of water and organic solvents with dissolved active substances generated in conventional processes. The scale-up of the $scCO_2$ impregnation-based processes has also become known in the last 20 years [20]. Grafting in the supercritical phase has been reported in the literature [21–25]. Correia et al. [22] developed a process of oligo(2-methyl-2-oxazoline) quaternized with *N*, *N*-dimethyldodecylamine synthesis and grafting to a chitosan scaffold in $scCO_2$. The obtained material, characterized by intense antibacterial activity, was proposed for water purification. Aminosilanes were successfully grafted to nanocellulose [24] to provide antibacterial activity and to CA, in our recent study [25], to provide antibiofilm properties. However, the materials grafted with aminosilanes may contain unreacted alkoxy groups prone to hydrolysis, and their application may be constrained. Xu et al. [23] reported the usage of $scCO_2$ in the chemical attachment of QACs to softwood using hexamethylene diisocyanate (HDI) as a linker via a carbamate/urethane linkage. The treated softwood showed improved dimensional stability and antibacterial activity [23].

Though QACs have long been known for their antibacterial properties [26], the antibiofilm properties of materials containing them are yet to be explored. A recent comprehensive review by Saverina et al. [27] summarizes the development of QACs and their antibacterial and antibiofilm activities when used alone, embedded in composites and coatings, or grafted to polymers. To the best of our knowledge, the first scientific report on CA grafting with QACs in the open literature is a conference proceeding [28] where we presented a part of the results from this study. A recent publication [29] dealing with CA-polyvinylpyrrolidone (CA-PVP) membrane modification by CA surface grafting with a QAC from a liquid solution also reported the antifouling potential of the obtained material.

This study presents a waterless process for obtaining a cellulose acetate-based biocidal polymer with strong antibiofilm properties for a broad spectrum of possible applications. Two QACs were synthesized and grafted via hexamethylene diisocyanate linker to cellulose acetate in $scCO_2$. Most of the published studies from the field investigate the antibacterial properties of materials against *Staphylococcus aureus* as a representative of Gram-positive bacteria and *Escherichia coli* as a Gram-negative. In this study, we extend the investigation of the antibiofilm properties of the obtained biocidal polymers to six bacterial species to gain broader insight into their bioactivity, which is expected to vary according to the different characteristics of investigated bacteria. Four statistical methods were applied to analyze the results, and statistical vs. microbiological significance was discussed.

2. Materials and methods

2.1. Materials and CA films production

Cellulose acetate (CA) Eastman CA-320S, in the form of beads, was a generous donation from Safic-Alcan, Poland. Hexamethylene diisocyanate (HDI, purity ≥98.0 %), dibutyltin dilaurate (purity 95 %), 11-bromo-1-undecanol (purity ≥99.0 %), N,N-dimethyltetradecylamine (purity ≥95 %), 2-dimethylaminoethanol (purity ≥99.5 %), 1-Bromoundecane (purity 98 %), Chloroform-D (purity 99.8 %), and cellulose acetate powder (CA, Mn ~ 30,000) were purchased from Sigma-Aldrich, Germany. Acetone (pure p.a.) was supplied by StanLab, Poland. 1-Propanol (pure p.a.) was provided by Chempur, Poland. Methanol (pure p.a.) and diethyl ether (pure p.a.) were purchased from POCH Avantor Performance Materials, Poland. Carbon dioxide (purity ≥ 99.5 %) was provided by SIAD, Poland.

Polymeric films were fabricated from CA powder by the solvent casting method. In a typical experiment, 0.25 g of CA powder was dissolved in 15 mL of acetone by stirring for two hours. The solution was poured into a Petri dish and left covered overnight for drying.

2.2. Quaternary ammonium compounds (QACs) synthesis and NMR analyses

2.2.1. Synthesis of N-(2-Hydroxyethyl)-N,N-dimethylundecan-1-aminium Bromide (QAC 1)

QAC 1 was synthesized from 2-dimethylaminoethanol and 1-bromoundecane (chemical reaction presented in Supplementary material, Fig. S1) according to the previously reported method [23,26]. 1.084 g of 2-dimethylaminoethanol was mixed with 3.171 g of 1-bromoundecane and refluxed at 80 °C for 30 min, resulting in the reaction mixture solidification. Subsequently, the mixture was cooled down to room temperature, followed by the addition of 6 mL of 1:3 (v/v) propanol: methanol for its complete dissolving. In the next step, the mixture was refluxed at 80 °C for 20 h. After removing the solvents by rotary evaporation, a whitish light substance was obtained. The substance was washed three times with diethyl ether and dried in vacuo, yielding a whitish powder.

2.2.2. Synthesis of N-(11-Hydroxyundecanyl-N,N-dimethyltetradecan- 1-aminium Bromide (QAC 2)

QAC 2 was synthesized from N,N-dimethyltetradecylamine and 11-bromo-1- undecanol (chemical reaction presented in Supplementary material, Fig. S2) according to the previously reported method [23,26]. 3.045 g of 11-bromo-1-undecanol was mixed with 3.350 g of N, N-dimethyltetradecylamine and refluxed at 80 °C for 30 min. The reaction mixture was subsequently cooled down to room temperature, followed by the addition of 6 mL of 1:3(v/v) 1-propanol:methanol. Subsequently, the reaction mixture was refluxed at 80 °C for 20 h, and cooled to room temperature. A white substance was obtained after removing solvents by rotary evaporation. The substance was washed three times with diethyl ether and dried in vacuo, yielding a white powder.

2.2.3. NMR analysis

1D (1 H, 13 C,) nuclear magnetic resonance spectroscopy spectra were recorded using NMR Bruker Avance 600 MHz with UltraShield Plus magnet (Billerica, Massachusetts, USA). The samples were prepared as follows: 20 mg of substance was dissolved in 700 µl of solvent ($CDCl_3$). 1 H and 13 C chemical shifts were referenced to tetramethylsilane (TMS; 0.0 ppm).

QAC 1: ^{1}H NMR (400 MHz, CHLOROFORM-*D*) *δ*: 0.85 (t, 3 H, $J = 6.8$ Hz, CH_3-11), 1.20 – 1.33 (m, 16 H, CH_2-3, CH_2-4, CH_2-5, CH_2-6, CH_2-7, CH_2-8, CH_2-9, CH_2-10), 1.75 (m, 2 H, CH_2-2), 3.34 (s, 6 H, CH_3-13, CH_3-14), 3.46 – 3.55 (m, 2 H, CH_2-1), 3.57–3.63 (m, 2 H, CH_2-15), 3.69–3.76 (m, 2 H, CH_2-16), 4.07–4.14 (m, 2 H, -OH-17). ^{13}C NMR (101 MHz, CHLOROFORM-*D*) *δ*: 14.2 (C-11), 22.7 (C-10), 22.9 (C-2), 26.3 (C-3), 29.31 (C-5), 29.38 (C-7), 29.4 (C-6), 29.5 (C-8), 29.6 (C-4), 31.9 (C-9), 52.2 (C-13, C-14), 55.9 (C-16), 65.7 (C-1), 66.2 (C-15). Mol. Wt.: 324.35 g/mol.

QAC 2: ^{1}H NMR (400 MHz, CHLOROFORM-*D*) *δ*: 0.83 (t, 3 H, $J = 6.7$ Hz, CH_3-15), 1.18 – 1.38 (m, 34 H, CH_2-4, CH_2-5, CH_2-6, CH_2-7, CH_2-8, CH_2-9, CH_2-10, CH_2-11, CH_2-12, CH_2-13, CH_2-18, CH_2-19, CH_2-20, CH_2-21, CH_2-22, CH_2-24, CH_2-25), 1.45–1.57 (m, 4 H, CH_2-14, CH_2-23), 1.59 – 1.72 (m, 4 H, CH_2-3, CH_2-17), 2.51 (s, 1 H, -OH), 3.34 (s, 6 H, CH_3-27, CH_3-28), 3.46 (td, $J = 10.7$, 6.8 Hz, 4 H, CH_2-2, CH_2-16), 3.57 (t, $J = 6.7$ Hz, 2 H, CH_2-26). ^{13}C NMR (101 MHz, CHLOROFORM-*D*) *δ*: 14.19 (C-15), 22.74 (C-14), 22.83 (C-3), 22.86 (C-17), 25.74 (C-4), 26.24 (C-24), 26.33 (C-18), 29.13 (C-6), 29.23 (C-20), 29.26 (C-12, C-23), 29.31 (C-11), 29.39 (C-8), 29.41 (C-22), 29.46 (C-7), 29.54 (C-5), 29.66 (C-9), 29.70 (C-10, C-19), 29.73 (C-21), 31.97 (C-13), 23.79 (C-25), 51.33 (C-27, C-28), 62.78 (C-26), 63.97 (C-2, C-16). Mol. Wt.: 492.67 g/mol.

2.3. Grafting in supercritical carbon dioxide

The isocyanate linker was grafted to cellulose acetate (CA) in the first step. CA beads and films were grafted in a 25 mL volume high-pressure view cell (Eurotechnica, Bargteheide, Germany), equipped with a heating jacket and thermostat. 1.4 mL of Hexamethylene diisocyanate (HDI), 0.2 mL of dibutyltin dilaurate, and 0.6 g of CA (beads or film) put in a filter bag were placed in the view cell. After the reactor was sealed, carbon dioxide was introduced up to the CO_2 cylinder pressure (~5.5 MPa). The view cell was subsequently heated to 70 °C. In the next step, the pressure was increased to 30 MPa by an air-driven gas booster (Eurotechnica GmbH, Bargteheide, Germany). The reaction was performed at 70 °C and 30 MPa for 6 h, followed by a moderate decompression rate of 0.33 MPa/min.

In the second step, QAC was attached to the linker-modified CA. Approximately 0.6 g of HDI – functionalized CA was put in a filter bag. The sample and 0.4 g of synthesized QAC were placed in the view cell. After the reactor was sealed, carbon dioxide was introduced to equalize with the CO_2 cylinder pressure. The view cell was heated to 70 °C, and subsequently, the pressure was increased to 30 MPa. The reaction was performed under the same conditions as the linker grafting (70 °C, 30 MPa, 6 h, and decompression rate 0.33 MPa/min).

After each grafting stage, the product was cleaned with ethanol and a paper towel. The reaction parameters selection (pressure, temperature, and time) for both steps was based on preliminary experiments, whereby FTIR analyses followed the grafting outcome. Compared to softwood, where the temperature of 100 °C, the pressure of 41.4 MPa, and the time of 20 h were employed [23], CA grafting was shown to be faster and attainable under milder conditions.

The product's mass change in both steps was followed by an analytical balance, and the grafting yield (Y) was calculated as

$$Y = \frac{W - W_0}{W_0} \bullet 100\% \quad (1)$$

where W is the mass of grafted polymer, and W_0 is its initial mass.

2.4. Characterization methods

The Fourier-transform infrared (FTIR) spectroscopy analysis was performed for chemical characterization of the neat and grafted polymer. The spectra were recorded in the ATR mode employing Nicolet iS50 Spectrometer (Thermo Fisher SCIENTIFIC, Waltham, MA, USA) with a resolution of 4 cm^{-1} at wavenumbers in the range of 500–4000 cm^{-1}.

Neat and grafted polymeric film hydrophilicity was followed using a goniometer model OCA 15EC (DataPhysics, Filderstadt, Germany) by measuring the water contact angle. DataPhysics' picolitre dosing system (PDDS) allows for reproducibly dosed droplets of down to 30 picolitres. The water drop was recorded by a camera, and the contact angle was analyzed upon the contact and after 3, 6, 9, and 12 s of the contact time.

The structural properties of neat and grafted polymer beads were investigated by scanning electron and ion beam microscopy. A two-beam microscope SEM/Ga-FIB FEI Helios NanoLab™ 600i (FEI, Thermo Fisher Scientific, Eindhoven, The Netherlands), equipped with ultra-high resolution electron and ion microscopy, was used. Energy focused beam of gallium ions was applied to perform cross-sections by the selective removal of the sample material. Before the analyses, the samples were coated with gold.

Differential scanning calorimetry (DSC) analysis was performed in a differential scanning calorimeter (Q10, TA Instruments, New Castle, DE, USA) previously described in detail [30]. The sample was heated at 10 °C/min from the room temperature of 25–300 °C under a nitrogen atmosphere with a gas flow rate of 50 mL/min to avoid oxidation reactions. The samples of the initial weight of 10 mg were placed in a hermetically sealed aluminum pan and measured three times. The desorption temperature (T_d), glass transition temperature (T_g), and melting temperature (T_m) were obtained by the DSC. The crystallinity degree was calculated as the ratio between the melting enthalpy of the material under study (ΔH_m) and the respective value for totally crystalline CA material (ΔH°_m) using the following formula: χc (%) $= \Delta H_m/\Delta H^\circ_m$ X 100, where $\Delta H^\circ_m = 58.8$ J/g as proposed by Cerqueira et al. [31] and Sousa et al. [32].

The mechanical properties of neat and grafted beads were screened by measuring the compression force that caused beads deformation using IMADA Force Gauge with stand MX2–500 N (IMADA. CO. LTD, Japan). Five measurements per sample were performed, and the force was expressed as mean ± standard deviation.

2.5. Microbiological investigations

2.5.1. Anti-attachment/antibiofilm effect of polymers

Investigations were performed on *Bacillus* (*B.*) *cereus* ATCC 11778, Methicillin-resistant *Staphylococcus* (*S.*) *aureus*, (MRSA) ATCC43300, *S. aureus* ATCC 29213, *Listeria* (*L.*) *monocytogenes* ATCC 13932, *E. coli* ATCC 10536, and *Salmonella* (*S.*) Enteritidis (*Salmonella enterica* subspecies *enterica* serovar Enteritidis) ATCC 13076 (Microbiologics, St. Cloud, MN, USA). All strains were first tested for the ability to produce

biofilms and, based on the obtained results (unpublished), were categorized as strong biofilm producers except for the *L. monocytogenes* ATCC 13932, which was a moderate biofilm producer. The selection of strains was based on their importance in medicine (biomedical devices) as well as in the food and water industry. The previously described assay of microbial adhesion to the polymer [8,25] was used. It was modified for microtiter plates with 96 flat bottom wells (neoCulture Cell and Tissue Culture Plates W96, No. C-8206, neoLab Migge GmbH, Heidelberg, Germany). Before testing, the strains were cultured for 24 h in Cation adjusted Mueller Hinton broth (CAMHB, Becton Dickinson, Heidelberg, Germany) with the addition of 1% glucose (Merck, KGaA, Darmstadt, Germany) to stimulate the production of exopolysaccharides important for attachment and biofilm production [8]. The polymer beads were sterilized in an autoclave at 121 °C, 120 kPa. Microtiter plate wells were filled with 100 μL of Tryptone Soya Broth (CM0129, Oxoid Ltd., Basingstoke, Hampshire, United Kingdom), and the polymer beads from each type (CA, CA-HDI-QAC1, CA-HDI-QAC2) were inserted into wells. Each polymer bead had a surface area of approximately 18 mm^2, therefore, the beads were grouped into groups of 3 (one sample consisted of 3 beads) in order to increase the surface area for possible attachment. Initial bacterial inoculum of 1–2 × 10^8 CFU/mL (OD600 0.08–0.1, Spectrofotometer Genesys 10-S, Thermo Fisher Scientific, Waltham, Massachusetts, United States) has been prepared, diluted to 1–2 × 10^6 CFU/mL, and 10 μL of such suspension was inoculated in investigated wells (final incolum 1–2 ×10^5 CFU/mL). Incubation was performed at 37 °C for 24 h. After this, the polymer beads were asepticaly removed, washed thoroughly with sterile Ringer's solution (112 mM NaCl, Merck KGaA, Darmstadt, Germany; 6 mM KCl, Chempur, Piekary Śląskie, Poland; 2 mM $CaCl_2$, Eurochem BGD, Tarnów, Poland; 1 M $NaHCO_3$ Eurochem BGD, Tarnów, Poland) to remove the planktonic cells from the surface, and then inserted into sterile 50 mL Eppendorf Tubes® BioBased, with screw caps, with 10 mL Ringer's solution and sonicated in an ultrasonic bath (37,000 Hz, Elmasonic S60, Elma Schmidbauer GmbH, Singen, Germany) at 5 s/min, for a total duration of 5 min. After completed sonication, the test tube in which the sonication was performed was considered a 10^{-1} dilution. From there, further serial dilutions from 10^{-2} to 10^{-7} were made. From each dilution, 100 μL were inoculated on the appropriate nutrient medium in three replicates: *L.monocytogenes* on 5 % sheep blood agar (Becton Dickinson, Heidelberg, Germany), *E.coli* and *Salmonella* spp., on MacConkey agar (Becton Dickinson, Heidelberg, Germany), *B. cereus*, MRSA and *S.aureus* on Trypton soya agar (Tryptone Soya Broth, CM0129, Oxoid Ltd., Basingstoke, Hampshire, United Kingdom, 1.2 % Agar Bacteriological (Agar NO. 1, LP0011, Oxoid Ltd., Basingstoke, Hampshire, United Kingdom). Plates were incubated at 37 °C for 48–72 h. The entire experiment was repeated in three independent replicates. The protocol for counting and recalculating the total number of CFU/mL was performed according to the ISO 7218 standard [33]. Only plates on which at least 15 and at most 300 colonies grew were used. The translation from the number of CFU/mL obtained in the dilutions into the total CFU/mm^2 of the polymer from which the bacteria were detached by ultrasound was performed using the formula:

$$NP = \frac{NCFU \bullet V}{P} \quad (2)$$

NCFU is the total number of detached bacteria (previously determined as CFU/mL), V is the volume of Ringer solution in tubes where ultrasonic detachment has been performed, and P is the total surface in mm^2 of the polymer.

2.5.2. Investigation of the antibacterial effect of polymers in the broth culture (influence on the multiplication and reduction of the total number of bacteria)

All materials and procedures described in sub Section 2.5.1 were applied in this part of the study. After the microtiter plates were incubated with the polymers and investigated strains, the polymer beads were removed, and the remaining broth cultures were serially diluted from 10^{-1} up to 10^{-8}. Inoculation and calculation of total number of bacteria (CFU/mL) were performed as described in Section 2.5.1.

2.5.3. Fixation of samples for SEM microscopy

Fixation of the attached strains after the polymer treatment in Tryptone soy broth inoculated with bacteria was performed according to the previously described procedure [8]. The polymers were kept for 30 min in 2.5 M Glutaraldehyde (Fluka Chemie GmbH, Buchs, Switzerland) previously dissolved in 0.5 M Sodium cacodylate buffer (Sigma-Aldrich, Darmstadt, Germany), then immersed in graded ethanol (ethanol/water 30/70, 50/50, 70/30, 90/10, 100, Avantor Performance Materials Poland S.A. (formerly POCH S.A.), Gliwice, Poland) for 15 min and finally for 30 s in Hexamethyldisilazane (99 %) (Sigma-Aldrich, Darmstadt, Germany).

2.5.4. Statistical methods

Descriptive and inferential statistical methods of hypothesis testing, i.e., regression analysis, analysis of variance (ANOVA), Tukey's Honest Significant Difference post hoc test, and Dunnett's test for multiple comparisons of different groups, were used. For the antimicrobial effect size quantification between polymer groups, Cohen's *d*, was used as a recommended test to follow ANOVA. The analyses were performed using the statistical software packages XLSTAT Version 2014.5.03., and IBM SPSS Version 26.0.0.0. In addition to the above tests, in order to monitor the effect of the investigated compounds on the growth and adhesion of microorganisms to surfaces, a logarithmic reduction was also calculated.

3. Results and discussion

3.1. QAC synthesis

Two QACs were synthesized and characterized by NMR and FTIR. To our knowledge, the only literature report on the synthesis of these compounds is provided by Xu et al. [23]. However, the authors [23] did not use these QACs for further work, and there is no data in the open literature on the biological activity of these particular QACs or their usage for material design purposes. The QAC 1 was synthesized with a yield of 80.8 %. Xu et al. [23] reported a 57.7 % yield. NMR and FTIR spectra of QAC 1 are presented in Fig. S3, and Fig. S4 (Supplementary material), respectively.

The QAC 2 was synthesized with a yield of 99.0 %. Xu et al. [23] reported a 95 % yield. NMR and FTIR spectra are presented in Fig. S5 and Fig. S6 (Supplementary material), respectively.

3.2. Grafting in supercritical carbon dioxide and material characterization

The grafting reactions in $scCO_2$ were performed at the pressure of 30 MPa and temperature of 70 °C. In the first step, the isocyanate linker reacted with hydroxyl groups of CA (Fig. 1). In the next step, QAC was attached to the linker via a carbamate/urethane linkage (Fig. 1).

The attachment of the isocyanate linker yielded a product weight increase of 10–13 %. In total, 19 experiments were performed. In the case of softwood, an increase of 30 % was reported [23]. FTIR spectra of pure and isocyanate grafted CA beads are presented in Fig. 2. In the spectrum of the neat CA bead, characteristic peaks of cellulose acetate are visible. The broad absorption band around 3460 cm^{-1} originates from O-H stretching of the hydroxyl group [34,35]. The peak at 1732 cm^{-1} is assigned to the stretching of the C═O group [30,35]. The bands at 1433, 1367, and 1220 cm^{-1} are attributed to the C-H bending, rocking, and wagging vibrations, respectively [30,36]. The peak at 1032 cm^{-1} is assigned to C-O-C linkage in the glycosidic unit, and the peak at 900 cm^{-1} is a characteristic of saccharide [30,37,38]. The spectra of the surface and cross-section of the linker grafted CA beads are

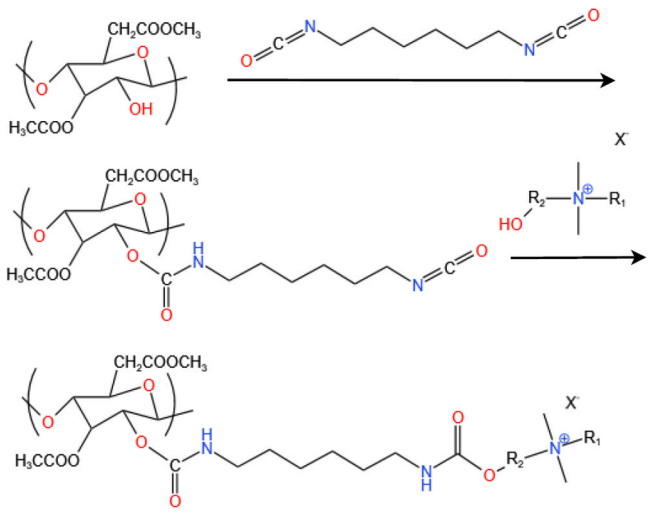

Fig. 1. Grafting of cellulose acetate with hexamethylene diisocyanate in the first, and with a QAC in the next reaction step.

presented in Fig. 2. The spectra are similar and show that the grafting reaction took place throughout the whole bead volume. The disappearance of the O-H stretching band of neat CA (3460 cm^{-1}) and the appearance of a new band at 3322 cm^{-1} originating from the stretching vibration of newly formed N-H bonds (Fig. 1) [23] is proof of successful grafting. The O-H stretching vibration of unreacted hydroxyl groups of the polymer also contributes to the observed band at 3322 cm^{-1} [23]. The new band at 2266 cm^{-1} is a typical contribution of the isocyanate group [39,40], which also proves the linker grafting. The new bands at 1619 and 1563 cm^{-1} originate from N-H bending vibrations, while the band at 1354 cm^{-1} is assigned to the C-N stretching vibration [40]. New bands at 2929 and 2856 cm^{-1} are assigned to the C-H asymmetric and symmetric stretching and the one observed at 1476 cm^{-1} to the C-H bending vibrations in grafted HDI [23,40,41].

The contact angle measurements are performed with CA films produced by the solvent-casting method using CA in powder form. The films were grafted with HDI and QACs in the same manner as CA beads. The results (Fig. 3) revealed increased hydrophobicity of CA films grafted with linker compared to pure CA film. Neat CA showed the contact angle with a water droplet around 74°. After the HDI attachment, the contact angle value was raised to 93.9°. Images of a water droplet on the films' surface at a predetermined time are presented in Fig. S7 (Supplementary material).

In the second step, QACs were attached to the previously grafted linker (Fig. 1). A slight product mass decrease, up to 2.8 %, was observed. Xu et al. [23] reported a reduction in softwood mass of 1.18 % after QACs' attachment. FTIR spectra of the polymer with attached QAC 1 and QAC 2 are presented in Fig. 4. The spectra show the isocyanate group being consumed completely (the peak at 2266 cm^{-1} disappeared), which is proof of the successful second grafting step (Fig. 1). Again, the grafting occurred throughout the whole polymer volume. The isocyanate group consumption is also visible in the spectra of QAC grafted beads' cross-section presented in Fig. S8 (Supplementary material). Contact angle measurements of grafted CA films showed a considerable hydrophobicity increase compared to pure CA film and CA film grafted with linker (Fig. 3, Fig. S7). As shown in Fig. 3 and Fig. S7 (Supplementary material), contact angles for films with attached QAC 1 and QAC 2 were around 107° and 113°, respectively (Fig. 3). Xu et al. [23] grafted two QACs, different than those in our study, to softwood using HDI as a linker. One of them provided similar hydrophobicity to the softwood surface as in our research, with a steady contact angle of 110°, while the attachment of the other QAC yielded a super hydrophilic surface [23].

Zhou et al. [29] produced CA-PVP membranes and performed CA

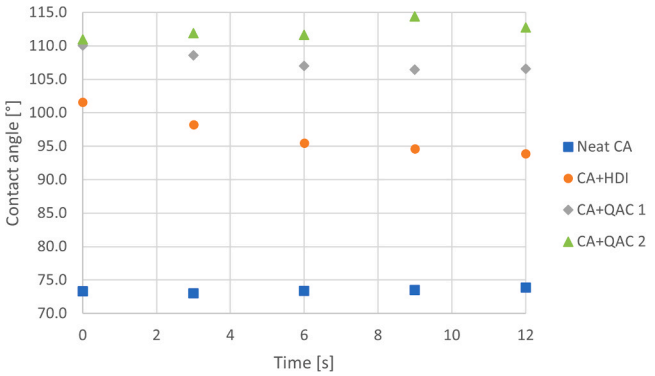

Fig. 3. Contact angle as a function of time for neat CA bead, CA bead grafted with linker (CA-HDI), and beads after the second grafting with QACs (CA-HDI-QAC 1 and CA-HDI-QAC 2).

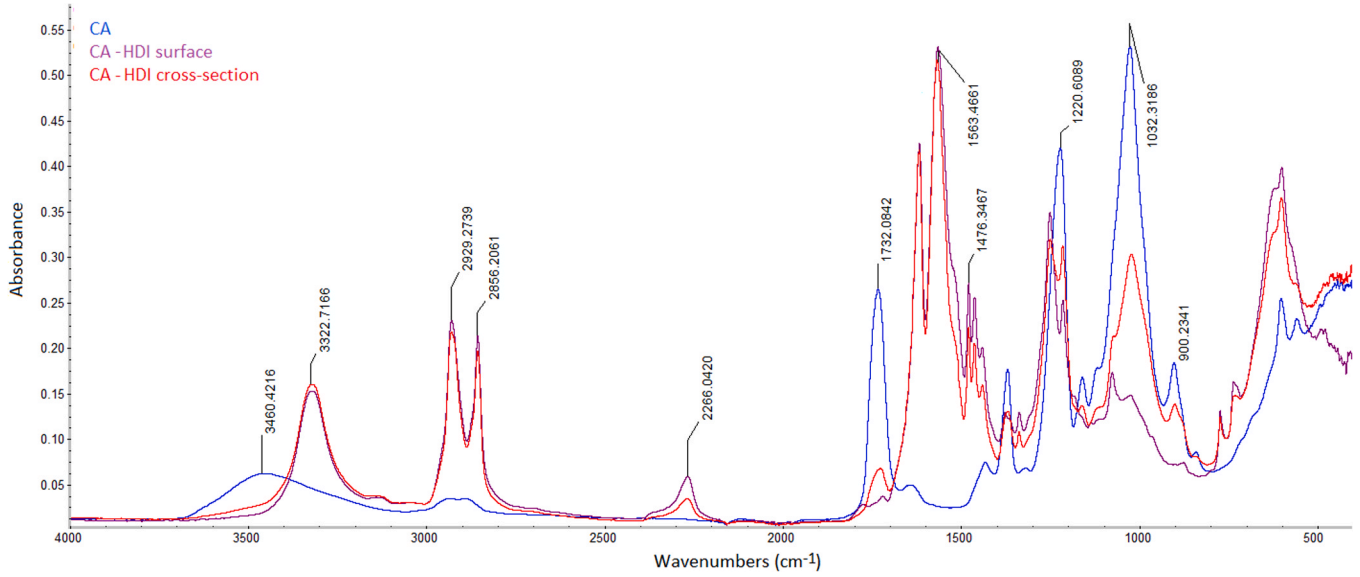

Fig. 2. FTIR spectra of neat (CA) and linker grafted (CA-HDI) cellulose acetate beads.

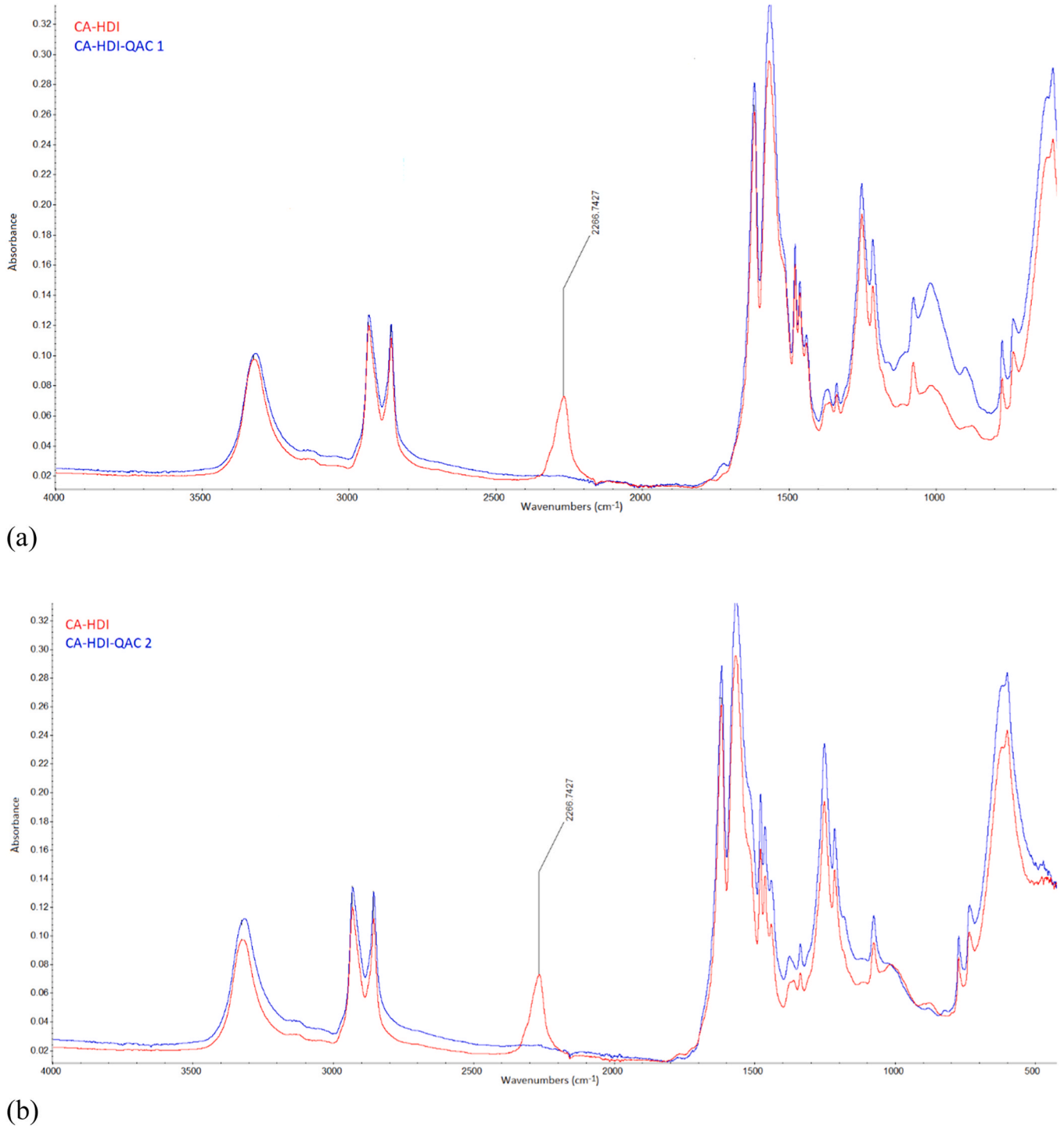

Fig. 4. FTIR spectra of the polymer with attached HDI and QAC 1 (a), and HDI and QAC 2 (b).

grafting with epoxy propyl dimethyl dodecyl ammonium chloride in a water solution. However, in the FTIR spectra, the authors haven't presented the part of the spectrum where the hydroxyl group absorption band of CA is expected (around 3460 cm^{-1}). Therefore, its potential disappearance due to successful grafting has not been presented as well. Taking into account the different chemical nature of used quaternary ammonium compounds, the spectra from their and our study can not be compared. The authors also reported increased hydrophilicity of the grafted material, while in our study, hydrophobic materials were obtained.

The grafting effects on the polymer morphology were followed by SEM-FIB microscopy. Besides the materials' surface, the cross-section was also studied by applying the energy-focused beam of gallium ions that allowed for sample cutting during the SEM investigation. The SEM images of the surface and cross-section of a neat CA bead and CA bead after the linker grafting are presented in Fig. 5 and Fig. 6., respectively. As can be seen, the grafting caused a change in the sample's surface. It became less smooth with "thread-like" aeries (Fig. 6(b) and (c)). The observed rugged surface is probably due to the lack of hydrogen bonding between polymer chains. Namely, hydroxyl groups of CA are responsible for the intermolecular hydrogen bonding between polymer chains. The reaction of hydroxyl groups in CA with the linker (HDI) (Fig. 1) yielded a

significant decrease in the number of hydroxyl groups available for ensuring this interaction between the polymer chains and contributed to the observed surface appearance. However, the linker grafted CA cross-section (Fig. 6d) revealed that the bead retained its compactness, even though the grafting occurred throughout its whole volume, as evidenced by the FTIR analysis (Fig. 2).

QAC attachment to the linker grafted material caused further morphology change. SEM images of beads with attached QAC 1 and QAC 2 are presented in Fig. 7 and Fig. 8, respectively. The investigated QACs yielded different appearances of product surfaces. The surface obtained after QAC 2 looked the most uneven with areas such as those presented in Fig. 8(a-c). However, the cross-section images of the QAC grafted beads (Fig. 7d and Fig. 8d) showed compact bead structures, though the QAC attachment occurred in the interior of the beads, as evidenced by the FTIR analysis (Supplementary material, Fig. S8).

The different thermal events taking place in the neat CA and modified CA (CA-HDI, CA-HDI-QAC 1, and CA-HDI-QAC 2) were evaluated using differential scanning calorimetry (DSC). The results are presented in Fig. 9 and Table 1. In the first stage, two endotherms are detected from room temperature to around 150 °C. The initial endotherms have minimum desorption temperatures (T_{d1}) and were attributed to the evaporation of acetic acid from the biopolymers [42]. The broad second endotherms (desorption temperatures T_{d2}) were attributed to the water desorption from the polysaccharide structure [32]. All curves have in common the presence of a broad endothermic event between 150 °C and 300 °C assigned to the melting of the crystalline regions of the polymer (melting temperatures T_m), and also exhibited low-intensity endothermic peaks corresponding to glass transition temperature (T_g). The DSC analysis showed a slight decrease in the glass transition temperature ranging from 225° to 223°C and an increased melting temperature between 248 and 278 °C due to the grafting (Table 1 and Fig. 9). The melting enthalpy decreased slightly after attachment of the linker and was significantly reduced after grafting the QACs. Similarly, the degree of crystallinity decreased from 15.5 % and 15.0 % after the first grafting step and further decreased to 4.1 % and 2.8 % after attaching QAC 1 and QAC 2, respectively. These results can be explained by the loss of the hydrogen bonding between biopolymer chains that existed in the neat CA due to the modification. The thermal properties analyzed by DSC also corroborate the ATR-FTIR and contact angle analysis, showing a clear distinction between pure CA, CA with the linker, and CA grafted with QACs.

The screening of the beads' mechanical properties showed that the linker grafting increased the resistance to deformation with the deformation force for pure CA, and CA-HDI of 114.7 ± 5.3 N and 192 ± 18 N, respectively. The second grafting step and the QACs attachment caused a decrease in beads' resistance to deformation compared to the linker grafted sample. The observed force values were 155 ± 25 N for CA-HDI-QAC 1 and 136.7 ± 14.3 N for CA-HDI-QAC 2, both higher than for the pure polymer.

3.3. Results of the microbiological investigations

3.3.1. Anti-attachment properties of CA, CA-HDI-QAC 1, and CA-HDI-QAC 2

The results of anti-attachment/antibiofilm abilities of the CA, CA-HDI-QAC 1, and CA-HDI-QAC 2 are shown in Table 2 and Fig. 10. The

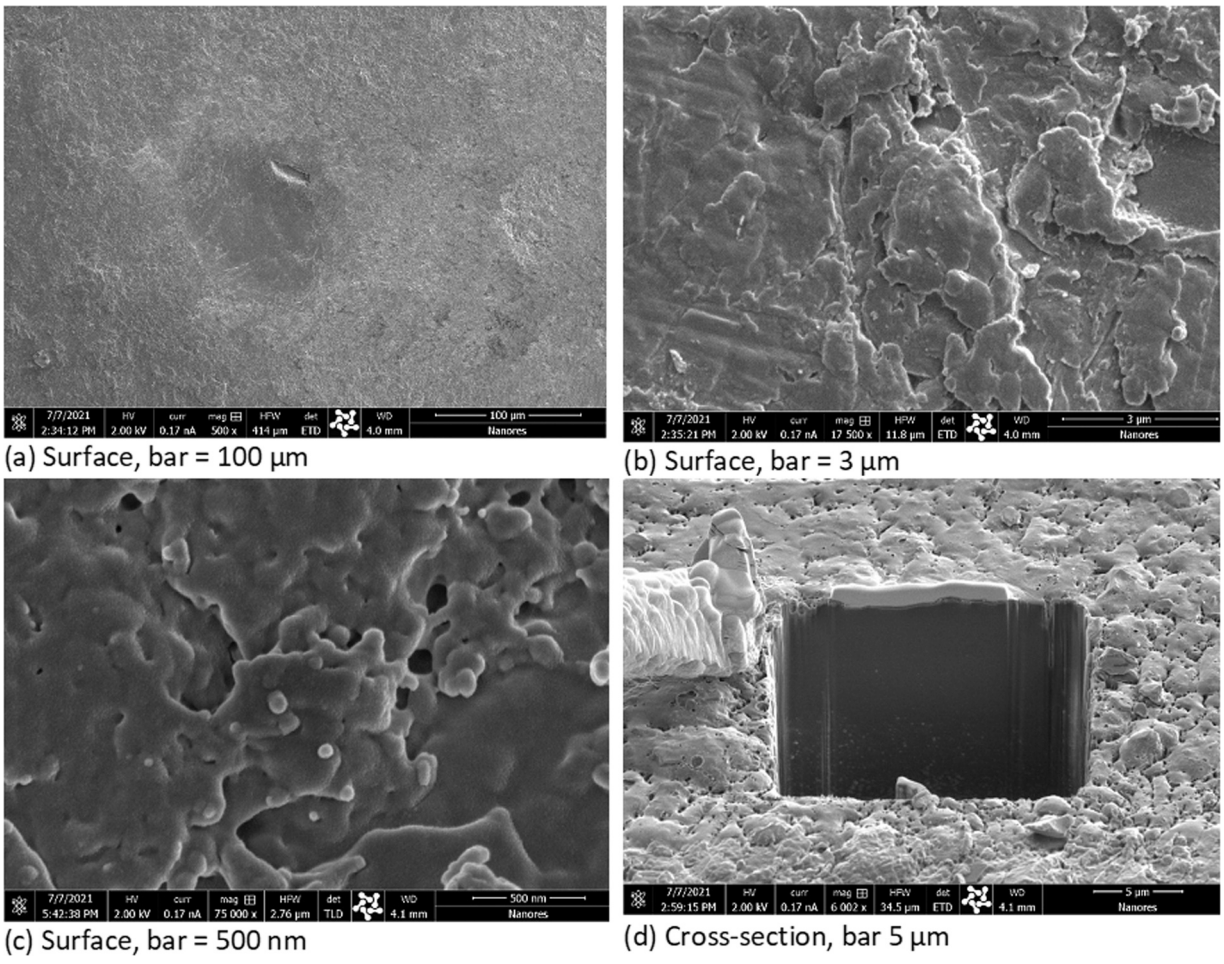

Fig. 5. SEM-FIB images of cellulose acetate bead (CA): surface (a), (b), and (c); cross-section (d).

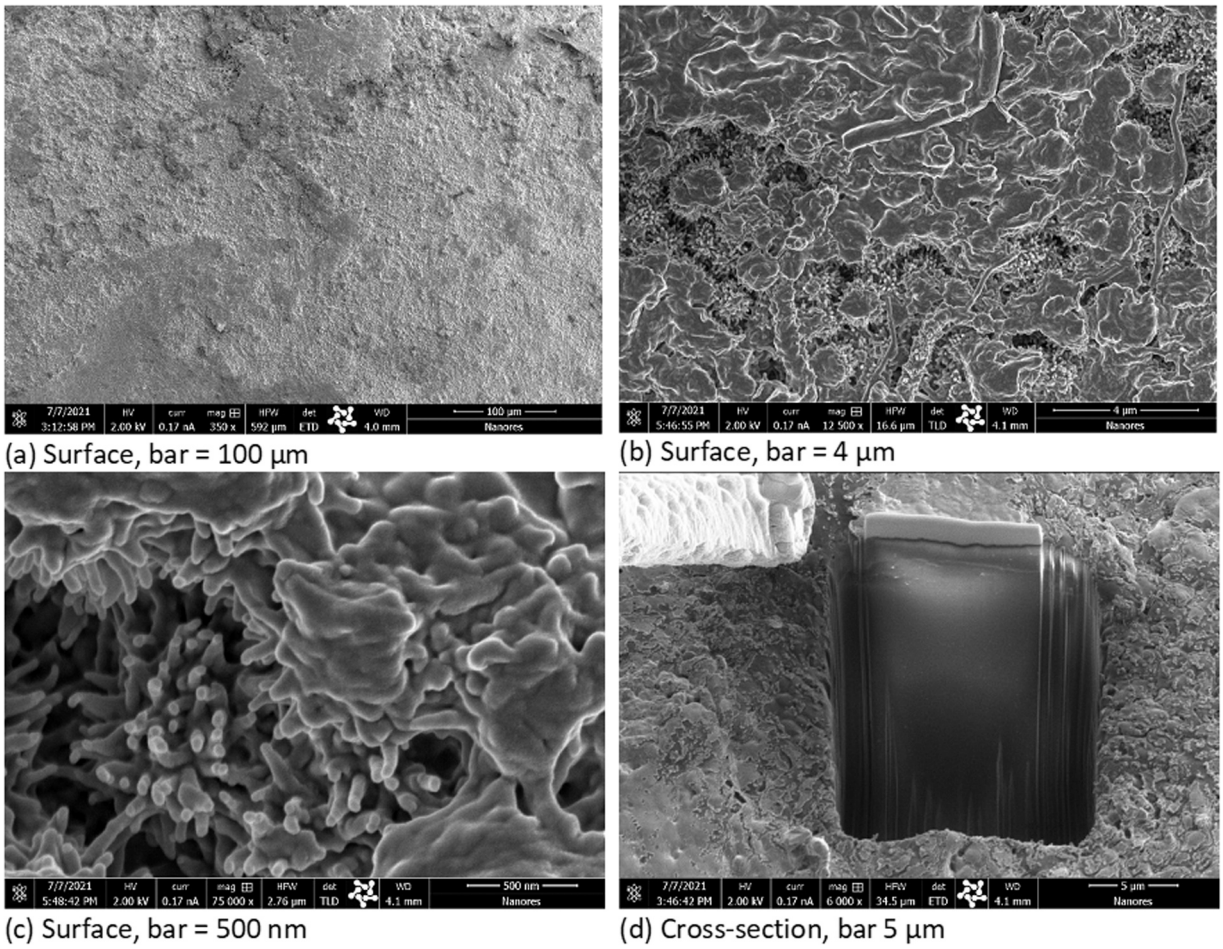

Fig. 6. SEM-FIB images of cellulose acetate bead grafted with the linker (CA-HDI): surface (a), (b), and (c); cross-section (d).

mean values obtained in three independent experiments are shown. Detailed statistical data are provided in the Supplementary material (Tables S1-S33).

All investigated strains showed statistically and microbiologically significant differences in their ability to adhere to CA-HDI-QAC2 and CA-HDI-QAC1 compared to CA.

E. coli ATCC 10536, *S*. Enteritidis ATCC 13076, *S. aureus* ATCC 29213, and MRSA ATCC 43300 were not capable of attaching to CA-HDI-QAC2 surface after 24 h of incubation in each of 3 independent experiments. *L. monocytogenes* ATCC 13932 attached in a total number of 4.75×10^6 CFU/mm^2 to the surface of CA, in a total number of 4.64×10^4 CFU/mm^2 to the surface of CA-HDI-QAC1 (2.01 log CFU reduction in relation to CA, R^2 =0.655, P = 0.0006), and in a total number of 4.44×10^3 CFU/mm^2 to the surface of CA-HDI-QAC2 (3.03 log CFU reduction in relation to CA, R^2 =0.655, P = 0.0007). *B. cereus* ATCC 11778 showed the highest ability to adhere to the surface of the tested polymers with the number of attached cells of 3.21×10^7 CFU/mm^2 on the surface of CA, 4.32×10^6 CFU/mm^2 on the surface of CA-HDI-QAC1 (0.87 log CFU reduction in relation to CA, R^2 =0.668, P = 0.0023), and the total number of $1{,}86 \times 10^5$ on the CA-HDI-QAC2 (2.24 log CFU reduction in relation to CA, P = 0.0003). *E. coli* ATCC 10536 had the highest ability to attach to CA-HDI-QAC1, it attached in an almost identical number as to the control CA (statistically nonsignificant 0.08 log CFU reduction, R2 =0.5489, P = 0.805, Cohen's *d* 0.15). The most susceptible to CA-HDI-QAC1 was MRSA, which was attached in a significantly reduced number compared to CA (1.34 log CFU reduction, R2 =0.7102, P = 0.0004, Cohen's *d* 1.15).

Polymer CA-HDI-QAC2 showed a clear and pronounced anti-attachment effect. The ability of *B. cereus* ATCC 11778 and *L. monocytogenes* ATCC 13932 to overcome the anti-adhesion activity of the CA-HDI-QAC2 and attach is attributed to their ability to adapt quickly.

Bacillus spp., and *Listeria* spp., do not have great importance in medical device-associated infections like *S.aureus*, although bacteremias caused by *Bacillus* species via medical devices have been reported in Japan [43]. However, *Bacillus* and *Listeria* spp. are used in the majority of biofilm studies because they are excellent biofilm producers capable of attaching and forming biofilms on surfaces where other bacteria cannot [44]. It has been reported that *L. monocytogenes* could easily adapt, multiply and form biofilms in the presence of sublethal doses of QACs [45]. Also, *B. cereus* produces a specific biosurfactant that enables it to adhere more easily and form biofilms in conditions where other bacteria perish, even in the presence of QACs [46].

The SEM investigation confirmed the results of the observed anti-adhesion effects. SEM images of surfaces of neat CA, CA-HDI-QAC 1, and CA-HDI-QAC 2 after exposure to MRSA ATCC 43300 strain are presented in Fig. 11. The surface colonization could be found at many places in the neat CA sample, as shown in Fig. 11a. At the surface of CA-HDI-QAC 1, no biofilm was found. However, planktonic cells could be sporadically spotted, as presented in Fig. 11b. At the same time, a bacteria-free surface of the CA-HDI-QAC 2 sample was observed (Fig. 11c).

We consider the most significant achievement of this study the impossibility of *S.aureus* ATCC 29213 and methicillin-resistant *S.aureus* ATCC 43300 to attach to the surface of the experimental polymer CA-HDI-QAC2. *S.aures* normally inhabit the skin of healthy people, and therefore, introducing this microorganism into the hospital environment is impossible to prevent [47]. Despite the implementation of all the

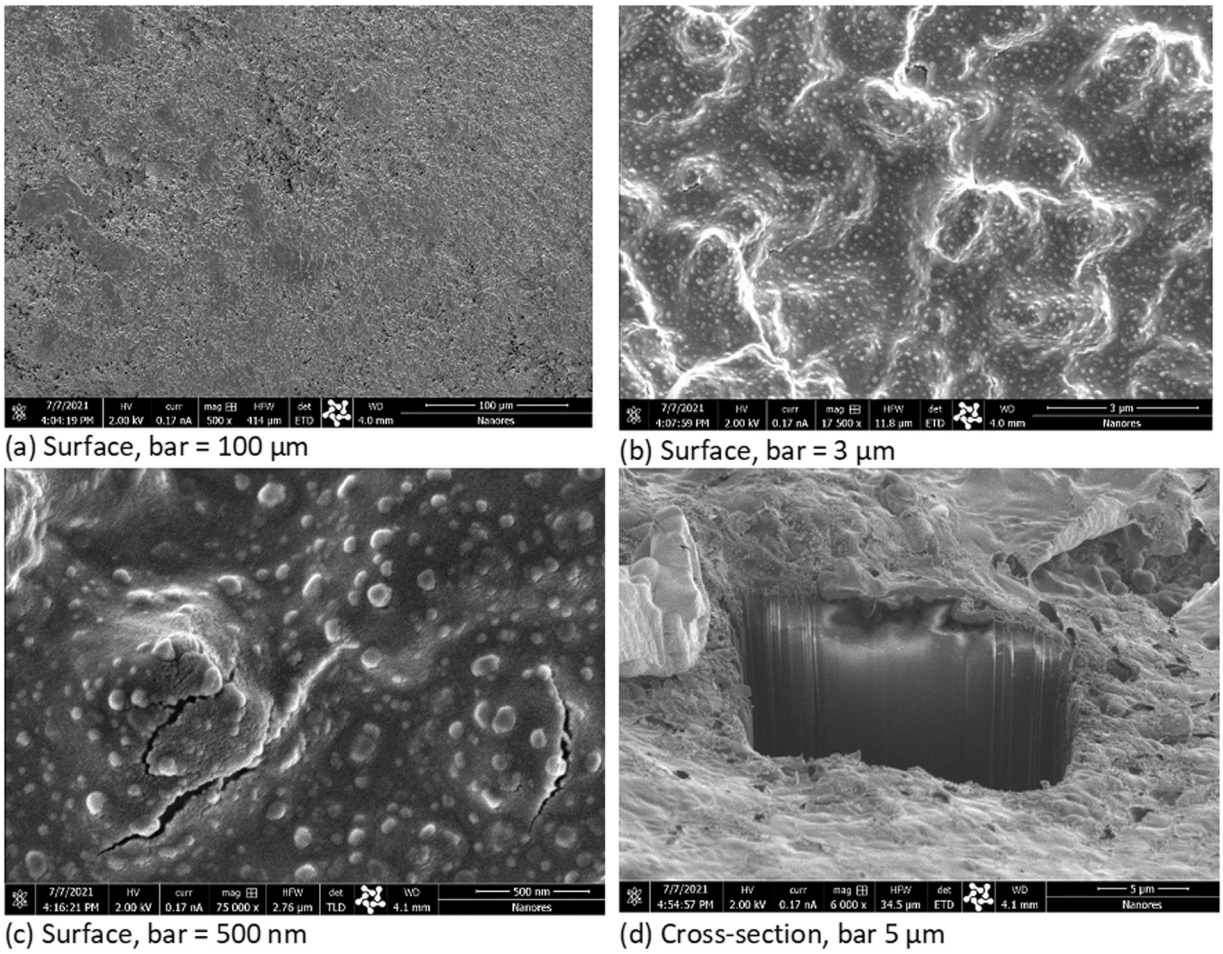

Fig. 7. SEM-FIB images of cellulose acetate bead grafted with QAC 1 (CA-HDI-QAC 1): surface (a), (b), and (c); cross-section (d).

possible precautionary measures of asepsis and antisepsis (UV radiation, sterilization, application of disinfectants, surgical glows, face masks), subsequent contamination of polymeric medical devices with staphylococci during manipulation, most often during the surgical process of insertion into the human body, is still a daily occurrence [8,47]. Staphylococci produce a whole spectrum of toxins and virulence factors, among which is their extraordinary ability to adhere to the surfaces of medical polymers and the production of highly resistant biofilms, which leads to a vast number of complications in patients with implanted medical aids [8]. Therefore, the most significant number of publications on this topic refers to *S.aureus*. To the best of our knowledge, this is the first report on biocide-grafted cellulose acetate against *B.cereus*, *L. monocytogenes,* and *S.* Enteritidis biofilms.

3.3.2. Influence of the CA, CA-HDI-QAC1 and CA-HDI-QAC2 on the multiplication of bacteria in the broth

The investigation aimed to check if there was QAC leaching from the material (the case of a significant effect on the multiplication in the broth) and to confirm QAC covalent bonding. The results of the influence of polymers on the multiplication of bacteria in the liquid medium are shown in Table 3 and Fig. 12. Polymer CA-HDI-QAC 2 influenced the multiplication of all investigated bacteria compared to pure broth, except for the *L. monocytogenes* ATCC13932, against which it was inert. The presence of CA-HDI-QAC 2 in the broth caused reduction of the total number of MRSA ATCC 43300 compared to pure medium (1.90 log CFU reduction, R^2 =0.816, $P < 0.0001$), and the weak reduction on *S.* Enteritidis (0.47 log CFU reduction, $R^2 = 0.92$, $P < 0.0001$) and *E. coli* ATCC 10536 (0,27 log CFU reduction, $R^2 = 0.946$, $P < 0.0001$).

Polymer CA-HDI-QAC1 also inhibited the multiplication of bacteria, including *L. monocytogenes* ATCC 13932, but with a weaker effect compared to CA-HDI-QAC 2. The weak reduction CA-HDI-QAC1 caused in MRSA ATCC43300 (0.49 log CFU reduction, $P < 0.0001$) followed by 0.29 log CFU reduction in *S. aureus* ATCC 29213 ($P < 0.0001$), 0.27 log CFU reduction in *E. coli* ATCC 10536 ($P < 0.0001$), and 0.23 log CFU reduction in *L. monocytogenes* ATCC 13932 ($P < 0.0001$).

Control polymer, pure cellulose acetate (CA), also affected the multiplication of bacteria. It had microbiologically very weak but statistically significant inhibitory effect on *S. aureus* ATCC 29213 (0.19 log CFU reduction, $R^2 = 0.925$, $P < 0.0001$, Cohen's *d* 2.56), and MRSA ATCC43300 (0.13 log CFU reduction, $p < 0.0001$, Cohen's *d* 0.91). It can be seen in Fig. 12 that CA also had a microbiologically weak but statistically significant effect on *L. monocytogenes* ATCC 13932, causing stimulation of multiplication of microorganism in comparison with the control pure medium (−0.50 log CFU, $R^2 = 0.841$, $P < 0.0001$, Cohen's *d* −9.80). A similar but statistically insignificant effect of stimulation of multiplication was also observed in *E. coli* ATCC 10536 (−0.03 log CFU, $P < 0.093$, Cohen's *d* −0.71).

The results indicate that materials showed microbiologically negligible suppression of bacterial multiplication in both [48], which most likely occurred only through direct contact of bacteria with the polymer. This finding testifies that QACs were covalently attached to cellulose acetate.

3.3.3. Statistical vs. microbiological significance

The partial discrepancy between statistical and microbiological significance in the obtained results in our study is a consequence of the rigidity of statistics that cannot fit into flexible, variable, highly adaptable, and unpredictable biological systems. In addition, microbiological

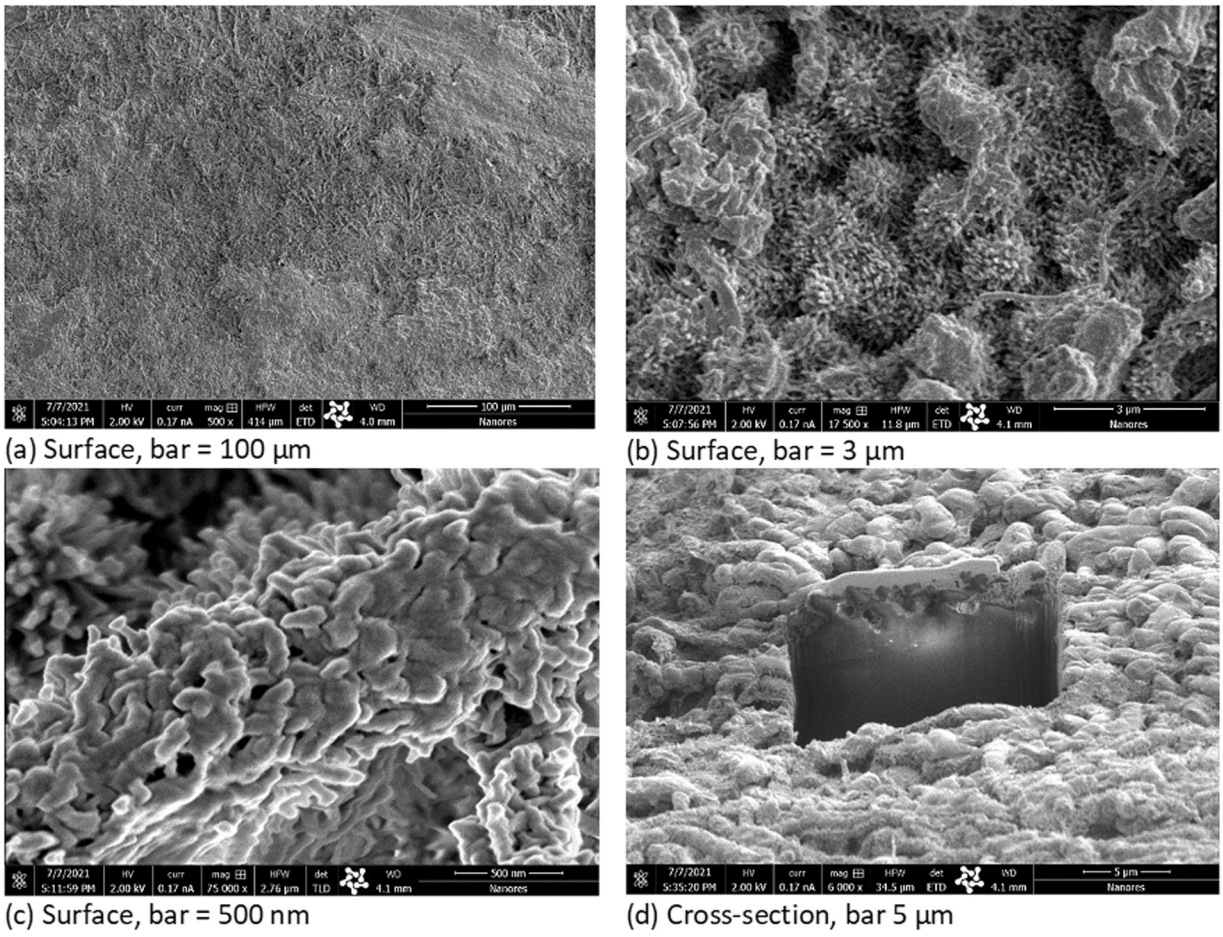

Fig. 8. SEM-FIB images of cellulose acetate bead grafted with QAC 2 (CA-HDI-QAC 2): surface (a), (b), and (c); cross-section (d).

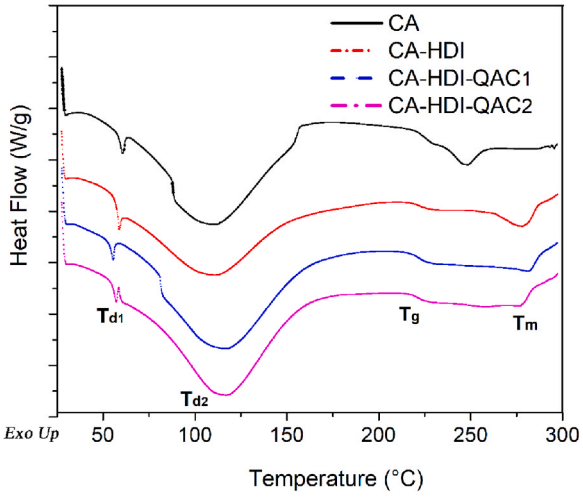

Fig. 9. Results of the DSC analysis of neat (CA) and grafted (CA-HDI, CA-HDI-QAC 1, and CA-HDI-QAC 2) beads.

criteria of "significance" are based mostly on the influence of microbiological results on human and veterinary medicine, food safety and sanitary principles, in contrast to statistical criteria based exclusively on numerical (mathematical) values. Thus, the obtained statistical results must be interpreted and accepted in the context of biological plausibility. To overcome this, we used four different statistical tests, which are shown in full in Tables 2 and 3, Supplementary material (Tables S1-S33), and Figs. 10 and 12. For example, in the results presented in Table 3 and S1-S19 (the influence of the CA, CA-HDI-QAC 1, and CA-HDI-QAC 2 on the multiplication of bacteria in the broth), the reduction in total CFU in investigated bacteria caused by CA-HDI-QAC1 ranged from 0.12 to 0.50 log CFU for all investigated strains, and it was statistically significant (ANOVA and post hoc test to test the significance of differences between groups). In microbiology, obtained reduction values are negligible. By microbiological criteria, a considerable reduction is only considered if equal to or greater than 3 log CFU compared to controls. The concentration of the antimicrobial substance and the time range in which this reduction occurred are also essential. Usually, 3 log CFU reduction obtained during 0–12 h (time-kill assay) at the lowest antimicrobial concentration is considered microbiologically significant [48]. This can be further commented on considering the results presented in Table 3. The total *E. coli* ATCC 10536 no. was reduced from 3.85×10^7 CFU/mL in pure medium to 2×10^7CFU/mL in the presence of polymer CA-HDI-QAC 2. In the microbiological sense, this reduction has neither clinical nor antimicrobial and food safety

Table 1
Results of DSC analysis for the neat and grafted polymer beads.

Sample	T_{d1} (°C)	T_{d2} (°C)	T_g (°C)	T_m (°C)	ΔH_m (J/g)	χ_c (%)
CA	60.8	110.1	224.9	247.8	9.1	15.5
CA-HDI	58.9	111.5	223.3	278.3	8.8	15.0
CA-HDI-QAC 1	55.5	115.8	223.1	282.0	2.4	4.1
CA-HDI-QAC 2	57.4	116.0	222.9	277.8	1.7	2.8

Table 2
Microbial attachment to CA, CA-HDI-QAC1 and CA-HDI-QAC2 expressed as the total number of colony forming units per mm^2 (CFU/mm^2).

Strain	Descriptive statistics	CA	CA-HDI-QAC 1	*Cohen's d*	CA-HDI-QAC 2	*Cohen's d*
***L. monocytogenes* ATCC 13932**	$\bar{x}$	4.75×10^6	4.64×10^4	0.95	4.44×10^3	0.96
	SD	4.95×10^6	4.94×10^4		7.70×10^3	
***B. cereus* ATCC 11778**	$\bar{x}$	3.21×10^7	6.48×10^6	0.88	1.86×10^5	1.09
	SD	2.91×10^7	2.00×10^5		1.61×10^5	
***E.coli* ATCC 10536**	$\bar{x}$	4.64×10^6	3.84×10^6	0.15	0	0.86
	SD	5.36×10^6	7.25×10^5		0	
***S.* Enteritidis ATCC 13076**	$\bar{x}$	1.67×10^5	2.83×10^4	1.03	0	1.24
	SD	1.35×10^5	5.00×10^3		0	
***S. aureus* ATCC 29213**	$\bar{x}$	5.23×10^6	2.37×10^5	1.10	0	1.15
	SD	4.53×10^6	9.67×10^4		0	
MRSA ATCC 43300	$\bar{x}$	2.04×10^6	5.80×10^4	1.03	0	1.06
	SD	1.93×10^6	5.12×10^4		0	

Legend: [1] Methicillin resistant *S. aureus*; * initial inoclum-1 $\times 10^5$ CFU/mL; $\bar{x}$- mean CFU/mL value obtained in three independent experiments; SD- standard deviation; Effect size (Cohen's *d*) was calculated by comparing the total CFU attached to CA-HDI-QAC1 and CA-HDI-QAC2 with the total CFU attached to CA.

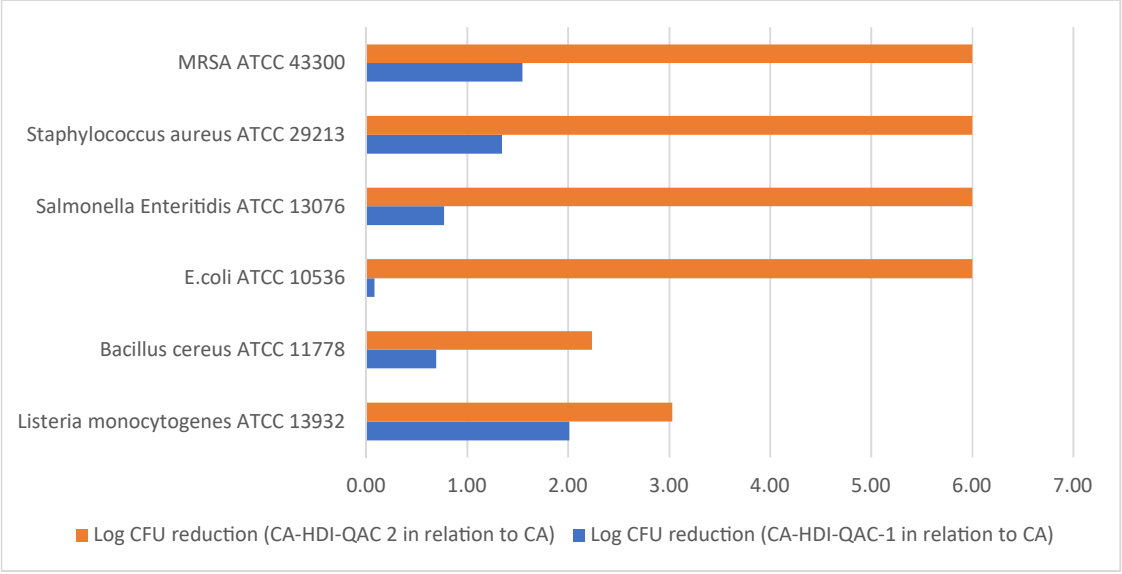

Fig. 10. Reduction of the total number of bacteria attached to CA-HDI-QAC1 and CA-HDI-QAC2 (calculated for 99.9% reduction for CA-HDI-QAC2) compared to CA, expressed as log CFU.

significance (very small or no effect, a huge number of bacteria is still present in the medium). Still, all statistical methods used in this study detected this reduction as significant. The aspect from which microbiological non-significance in this part of the research is best seen is the initial number of bacteria. *S.* Enteritidis ATCC 13076, multiplied from the initial 10^5CFU/mL to a level of 2×10^7 CFU/mL and 1.25×10^8 CFU/mL regardless of the presence of CA-HDI-QAC 1 and CA-HDI-QAC 2, respectively, compared to the control (pure medium), which is considered microbiologically negligible suppression, and it most likely occurred only through direct contact with the polymer. On the other hand, the microbiological and statistical significance fully agreed in the calculation of CFU reduction in the anti-attachment effect on CA-HDI-QAC 2 compared to CA. In all microorganisms, the obtained reduction was ≥ 3 log CFU.

3.3.4. Discussion on the biocidal activity of QAC grafted materials and the proposed process

The biocidal mechanism of a free QAC (including QAC released from the material) can be explained as follows [27]. The positively charged "head" of the QAC interacts with the surface of the membrane, thereby replacing the membrane-stabilizing Mg^{2+} and Ca^{2+} cations (ion exchange effect). The lipophilic part of the QAC is then embedded into the phospholipid bilayer. As a result, the membrane breaks, and the cytoplasmic material leaks out of the cell [27]. However, due to limited diffusion, the mechanism may change when QACs are covalently bound to a surface [27,49]. The first biocidal mechanism, the polymeric spacer effect, assumes the surface grafted poly-onium cations might penetrate the bacterial cell wall, reach the cell membrane, and disrupt the phospholipid bilayer, leading to intracellular constituents leakage and cell death. Lewis and Klibanov [50] showed that the molecular weight of *N*-alkylated polyethyleneimine immobilized on glass considerably affected the antimicrobial properties. The authors claimed the impact was due to the long-chain cationic polymer being able to penetrate the phospholipid membrane. However, the other types of QACs with much shorter chain lengths cannot operate by this mechanism [50,51]. The second biocidal mechanism, so-called phospholipid sponge effect, explains the grafted QAC activity by their positive charges causing electrostatic interactions strong enough to rip apart the negatively charged phospholipids from the cell membrane [49,51]. Gao et al. [49] prepared a surface-bound *N,N*-dodecyl methyl-co-*N,N*-methylbenzophenone methyl quaternary PEI (DMBQPEI) of different cross-linking densities. A negative correlation between the film cross-linking density and absorption of a negatively charged phospholipid was observed, but no such correlations were noticed with a neutral phospholipid (DPhPC), indicating the anionic phospholipid suction proposed by the mechanism. Moreover, the killing efficiency of the material on *S. aureus and E. coli* was inversely affected by the cross-linking density of the films, providing additional evidence for the phospholipid sponge effect.

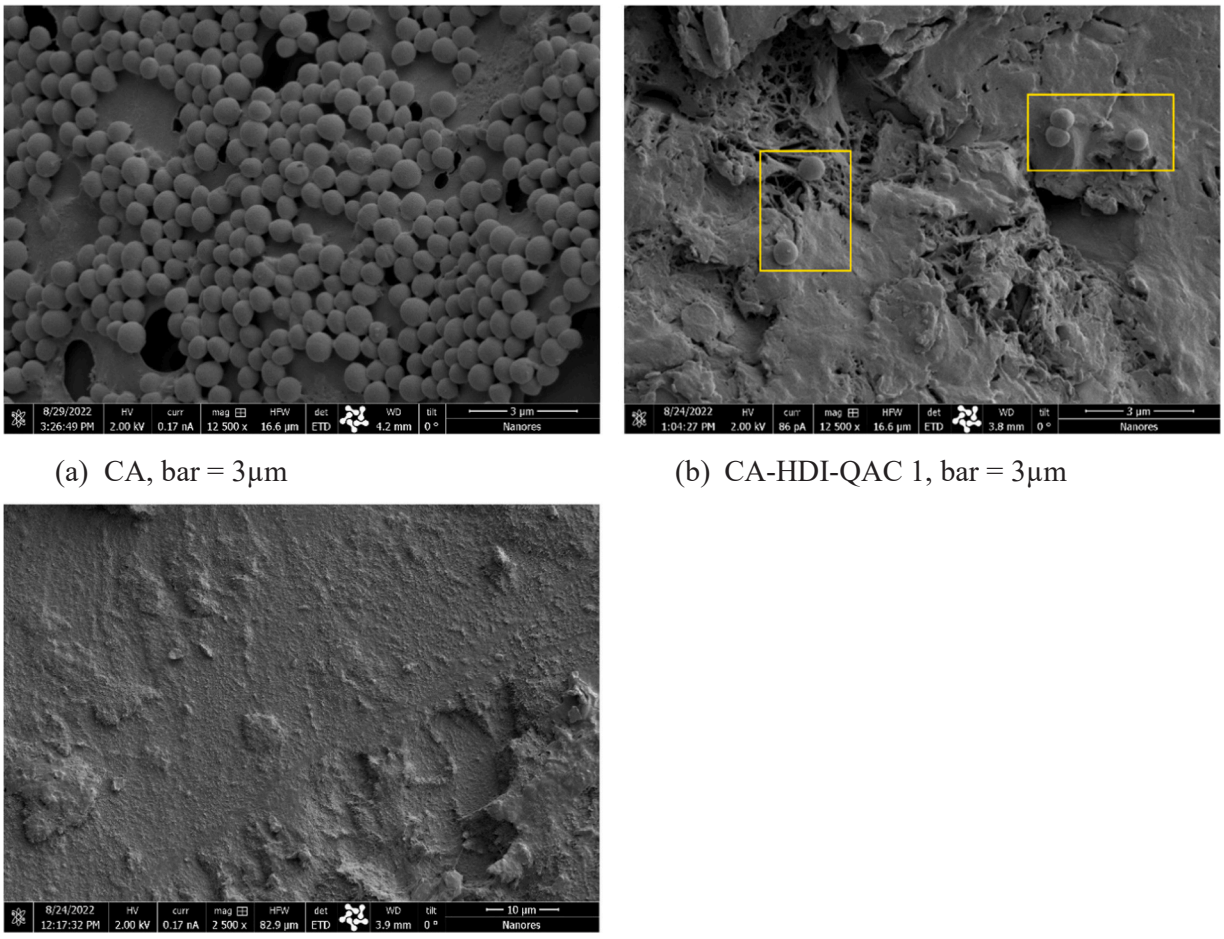

(a) CA, bar = 3µm

(b) CA-HDI-QAC 1, bar = 3µm

(c) CA-HDI-QAC 2, bar = 10 µm

Fig. 11. Polymer surfaces after exposure to MRSA ATCC 43300 strain. Neat CA (a), CA-HDI-QAC 1 (b), and CA-HDI-QAC 2 (c).

Table 3
Total number of bacteria (CFU/mL) after 24 h of incubation in Tryptone soy broth with the addition of CA, CA-HDI-QAC 1 and CA-HDI-QAC 2.

Strain	Descriptive statistics	Pure medium	CA	*Cohen's d*	CA-HDI-QAC 1	*Cohen's d*	CA-HDI-QAC 2	*Cohen's d*
***S. aureus* ATCC 29213** *	$\bar{x}$	7.43×10^7	4.76×10^7	2.56	3.82×10^7	3.47	1.98×10^6	6.94
	SD	1.04×10^7	1.43×10^7		1.81×10^7		3.97×10^5	
[1]MRSA ATCC 43300 *	$\bar{x}$	7.11×10^7	5.21×10^7	0.91	2.28×10^7	2.31	$8{,}96 \times 10^5$	3.35
	SD	2.09×10^7	1.01×10^7		3.74×10^7		8.38×10^5	
***S.* Enteritidis ATCC 13076** *	$\bar{x}$	1.25×10^8	1.24×10^8	0.07	7.60×10^7	2.32	4.28×10^7	3.89
	SD	2.12×10^7	1.57×10^7		2.14×10^7		7.44×10^6	
***E.coli* ATCC 10536** *	$\bar{x}$	3.85×10^7	4.165×10^7	-0.71	3.785×10^7	0.15	2.06×10^7	4.13
	SD	4.33×10^6	3.26×10^6		1.87×10^6		3.69×10^6	
***L. monocytogenes* ATCC 13932** *	$\bar{x}$	1.03×10^6	3.23×10^6	-9.80	6.11×10^5	1.85	1.02×10^6	0.05
	SD	2.25×10^5	1.56×10^6		1.51×10^5		1.76×10^5	
***B. cereus* ATCC 11778** *	$\bar{x}$	1.70×10^8	1.63×10^8	0.39	1.29×10^8	2.41	1.39×10^7	9.23
	SD	1.69×10^7	1.86×10^6		4.70×10^7		1.06×10^7	

Legend: [1] Methicillin resistant *S. aureus*; * initial inoclum-1×10^5 CFU/mL; $\bar{x}$- mean CFU value obtained in three independent experiments; SD- standard deviation; CV- variation coefficient. Effect size (Cohen's *d*) was calculated by individually comparing the total number of CFU in each broth in which QACs were added to the total number of CFU in pure broth.

Considering that materials synthesized in this study do not comprise a long-chain cationic polymer grafted on the surface like in the study of Lewis and Klibanov [50], or so-called polymer brushes [27], the polymeric spacer effect could be neglected. The most probable causes of the strong antibiofilm properties reported in this research are the combined ion exchange and phospholipid sponge effects. Namely, when bacteria come close to the positively charged grafted QACs, the bacterial membrane-stabilizing ions (Mg^{2+} and Ca^{2+}) are displaced to raise the entropy of the system [51]. The loss of these ions results in membrane disruption that further facilitates the phospholipid sponge effect.

However, most authors uniformly agree that the activity of QAC depends on the ability to penetrate the bacterial cell wall. In this sense, the ability of bacteria to quickly develop membrane adaptation mechanisms so that it becomes impermeable to the biocidal molecule (resistance) is possible [52]. In addition, the bacterium can be naturally insensitive to a QAC due to the natural impermeability of its membrane to QAC molecules (intrinsic resistance). Still, in our case, this mechanism can be excluded because all investigated strains showed

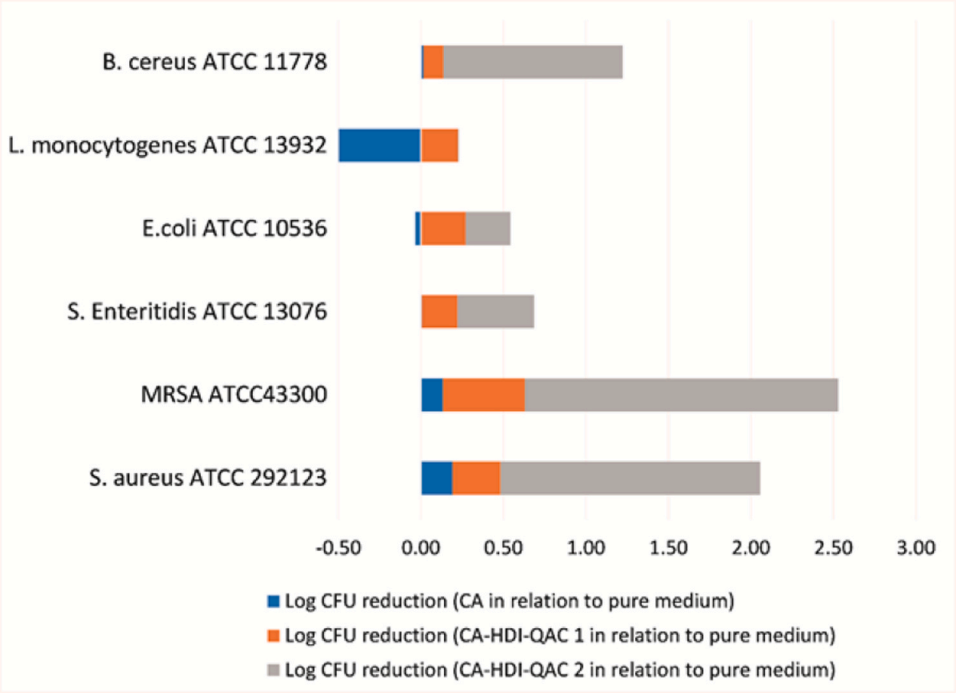

Fig. 12. Reduction of the total number of bacteria expressed as log CFU after 24 incubation in Tryptone soy broth with CA, CA-HDI-QAC 1, and CA-HDI-QAC 2. A negative log CFU value indicates increased proliferation compared to the control (pure) medium (related to *L. monocytogenes* ATCC 13932 and *E. coli* ATCC 10536).

susceptibility to grafted QACs to a greater or lesser extent. In the end, based on all norms of basic microbiology, the killed bacteria are most often instantly lysed and disintegrated and thus unable to attach any abiotic and biotic surfaces. Therefore, they must not be seen on the surface of antimicrobial materials, as demonstrated by the SEM image in Fig. 11c.

Zhou et al. [29], in their microbiologically non-reproducible [53] study, investigated the activity of CA grafted with epoxy propyl dimethyl dodecyl ammonium chloride, in a water solution, against *E. coli* and *S. aureus*, and reported antibacterial and anti-adhesion properties of the material. The authors did not present a single numerical value of the change in the number of bacteria per unit of the medium, per unit of material's surface, and per unit of time, based on which the repeatability of the experiment could be followed [53]. The authors inexplicably cultivated the tested strains for only 8 h, which according to available standards for testing the antimicrobial activity, is too short for the biological process of attaching bacteria to the material's surface, especially in anti-biofilm investigations [54–57]. It is considered that the optimal length of incubation in such studies should be minimum 24–72 h (unless it is a time-kill assay that is done every 2–4 h during 24 h) [8,25]. Furthermore, in the study [29], the tested initial bacterial inoculum amounted to only 100 μL per 1 cm^2 of the polymer, which is insufficient to submerge the material fully. For the anti-attachment property testing of polymers, at least 2–5 or 10 mL, and up to 50 mL of the medium are usually requested [58,59]. Finally, the authors claim to have proven a strong antibacterial effect of tested samples, but they failed to prove whether the active component is released into the medium or acts only by contact.

The process suggested in this study enabled the production of hydrophobic materials with strong antibiofilm properties in a waterless process, which is a significant improvement of the existing technologies. In addition to complete effluent elimination by the proposed process, the active component consumption is significantly reduced compared to the conventional processes, and its release into the environment is prevented. Using $scCO_2$, the unreacted QAC remains in the solid form and may be used in the next cycle. The scale-up of the impregnation process with $scCO_2$ is known [20], with industrial plants' size and investment costs depending on the product type and capacity. Industrial examples are wood impregnation [20,60], textile dyeing [20,61], and medical device production [20,62]. Based on the high-pressure vessel's size and the type of solid to be impregnated, special construction features might be necessary to ensure a homogeneous distribution of $scCO_2$ within the vessel [60]. The investment costs in the high-pressure equipment for $scCO_2$ applications are higher than in the conventional processes conducted under atmospheric pressure and range between several thousand euros for smaller vessels up to 50 dm^3, applicable to medical device impregnation and grafting reactions, to several million euros for industrial processes with several larger vessels [63,64]. On the other hand, energy consumption and operational costs are lower than in conventional processes due to the minimized consumption of chemicals, the absence of organic solvents and water usage, and the absence of a drying step [61]. When developing a new product, a cost-effective way is to start with small high-pressure equipment and then scale up the processes stepwise, combined with commercial and life cycle analysis [20].

Another advantage of $scCO_2$ impregnation and grafting is the possibility of modifying finished polymeric forms. Examples are hip and knee endoprosthesis impregnation [65,66], stent impregnation [62], as well as commercial polymeric membrane impregnation [67,68], and grafting [25]. Similarly, in the case of materials proposed in this study, the grafting of finished polymeric forms (fabricated items for particular applications) should be considered in further research.

4. Conclusions

N-(2-Hydroxyethyl)-N,N-dimethylundecan-1-aminium Bromide (QAC 1) and N-(11-Hydroxyundecanyl-N,N-dimethyltetradecan- 1-aminium Bromide (QAC 2) were synthesized and chemically attached to cellulose acetate using hexamethylene diisocyanate as a linker via a carbamate/urethane linkage, in supercritical carbon dioxide. Both grafting steps, the linker, and QACs attachment, were performed at 30 MPa and 70 °C for six hours and provided polymer modification throughout its whole volume. The reduced intensity of intermolecular interactions between the polymer chains due to the conversion of hydroxyl groups in the grafting reaction led to a decrease in the degree of

crystallinity and the appearance of a rugged polymer surface. However, the cross-section imaging revealed a compact polymer structure. The polymer surface showed hydrophobic properties with a stable contact angle of 106° and 112° for polymer grafted with QAC 1 and QAC 2, respectively. The examined polymers did not completely prevent the attachment of *B. cereus* ATCC 11778 and *L. monocytogenes* ATCC 13932. However, the aforementioned bacteria attached to CA-HDI-QAC 2 in microbiologically and statistically significantly smaller numbers than to control CA. Indeed, the most important result of the study is the complete impossibility of *S.aureus* ATCC 29213 and MRSA ATCC 43300 attachment to CA-HDI-QAC 2 polymer, as equally obtained in three independent experiments. Similarly, neither *E.coli* ATCC 10536 nor *S.* Enteritidis ATCC 13076 were able to attach to CA-HDI-QAC 2. It can be concluded that the polymer CA-HDI-QAC 2 showed excellent anti-attachment properties against all tested strains. Such material, obtained in an effluent-free process, is of interest for application in the production of medicinal devices, membranes for water treatment units, bioreactors, piping and vessels for the food industry, and active surfaces for hospital applications and biofouling control.

CRediT authorship contribution statement

Mariusz Nowak: Investigation, Validation, Visualization, Writing – original draft. **Damian Semba**: Investigation. **Dusan Misic**: Methodology, Investigation, Conceptualization, Supervision, Writing – original draft. **Tomasz Pólbrat**: Investigation. **Dusica Stojanovic**: Investigation. **Slavoljub Stanojevic**: Formal Analysis. **Anna Trusek**: Resources. **Irena Zizovic**: Conceptualization, Methodology, Investigation, Supervision, Funding Acquisition, Writing – review & editing.

Declaration of Competing Interest

The authors declare that they have no known competing financial interests or personal relationships that could have appeared to influence the work reported in this paper.

Data availability

Data will be made available on request.

Acknowledgments

The research was funded by Narodowe Centrum Nauki, (Poland), grant number 2018/31/B/ST8/01826. The financial support is gratefully acknowledged.

Appendix A. Supporting information

Supplementary data associated with this article can be found in the online version at doi:10.1016/j.supflu.2023.106058.

References

[1] E.-R. Kenawy, S.D. Worley, R. Broughton, The chemistry and applications of antimicrobial polymers: a state-of-the-art review, Biomacromolecules 8 (2007) 1359–1384, https://doi.org/10.1021/bm061150q.
[2] M. Berlanga, R. Guerrero, Living together in biofilms: the microbial cell factory and its biotechnological implications, Microb. Cell Factor. 15 (2016), 165, https://doi.org/10.1186/s12934-016-0569-5.
[3] K.W.K. Lee, S. Periasamy, M. Mukherjee, C. Xie, S. Kjelleberg, S.A. Rice, Biofilm development and enhanced stress resistance of a model, mixed-species community biofilm, ISME J. 8 (2014) 894–907, https://doi.org/10.1038/ismej.2013.194.
[4] M. Burmølle, D. Ren, T. Bjarnsholt, S.J. Sørensen, Interactions in multispecies biofilms: do they actually matter? Trends Microbiol. 22 (2014) 84–91, https://doi.org/10.1016/j.tim.2013.12.004.
[5] I. Francolini, G. Donelli, Prevention and control of biofilm-based medical-device-related infections, FEMS Immunol. Med. Microbiol. 59 (2010) 227–238, https://doi.org/10.1111/j.1574-695X.2010.00665.x.
[6] Y.M. Wi, R. Patel, Understanding biofilms and novel approaches to the diagnosis, prevention, and treatment of medical device-associated infections, Infect. Dis. Clin. North Am. 32 (2018) 915–929, https://doi.org/10.1016/j.idc.2018.06.009.
[7] A. Mahapatra, Study of biofilm in bacteria from water pipelines, J. Clin. Diagn. Res. (2015), https://doi.org/10.7860/JCDR/2015/12415.5715.
[8] G. Donelli, Microbial Biofilms: Methods and Protocols, Humana Press; Springer,, New York, 2014.
[9] J. Puls, S.A. Wilson, D. Hölter, Degradation of cellulose acetate-based materials: a review, J. Polym. Environ. 19 (2011) 152–165, https://doi.org/10.1007/s10924-010-0258-0.
[10] E.N. Bifari, S. Bahadar Khan, K.A. Alamry, A.M. Asiri, K. Akhtar, Cellulose acetate based nanocomposites for biomedical applications: a review, Curr. Pharm. Des. 22 (2016) 3007–3019, https://doi.org/10.2174/1381612822666160316160016.
[11] M. Fornazier, P. Gontijo De Melo, D. Pasquini, H. Otaguro, G.C.S. Pompêu, R. Ruggiero, Additives incorporated in cellulose acetate membranes to improve its performance as a barrier in periodontal treatment, Front. Dent. Med. 2 (2021), 776887, https://doi.org/10.3389/fdmed.2021.776887.
[12] R. Konwarh, N. Karak, M. Misra, Electrospun cellulose acetate nanofibers: The present status and gamut of biotechnological applications, Biotechnol. Adv. 31 (2013) 421–437, https://doi.org/10.1016/j.biotechadv.2013.01.002.
[13] Y. Liu, Q. Wang, Y. Lu, H. Deng, X. Zhou, Synergistic enhancement of cytotoxicity against cancer cells by incorporation of rectorite into the paclitaxel immobilized cellulose acetate nanofibers, Int. J. Biol. Macromol. 152 (2020) 672–680, https://doi.org/10.1016/j.ijbiomac.2020.02.184.
[14] A.M. Pandele, P. Neacsu, A. Cimpean, A.I. Staras, F. Miculescu, A. Iordache, S. I. Voicu, V.K. Thakur, O.D. Toader, Cellulose acetate membranes functionalized with resveratrol by covalent immobilization for improved osseointegration, Appl. Surf. Sci. 438 (2018) 2–13, https://doi.org/10.1016/j.apsusc.2017.11.102.
[15] I. Zizovic, Supercritical fluid applications in the design of novel antimicrobial materials, Molecules 25 (2020) 2491, https://doi.org/10.3390/molecules25112491.
[16] G. Brunner, Applications of supercritical fluids, Annu. Rev. Chem. Biomol. Eng. 1 (2010) 321–342, https://doi.org/10.1146/annurev-chembioeng-073009-101311.
[17] M. Perrut, Supercritical fluid applications: industrial developments and economic issues, Ind. Eng. Chem. Res. 39 (2000) 4531–4535, https://doi.org/10.1021/ie000211c.
[18] Ž. Knez, E. Markočič, M. Leitgeb, M. Primožič, M. Knez Hrnčič, M. Škerget, Industrial applications of supercritical fluids: a review, Energy 77 (2014) 235–243, https://doi.org/10.1016/j.energy.2014.07.044.
[19] M.A. Fanovich, P. Jaeger, Sorption and diffusion of compressed carbon dioxide in polycaprolactone for the development of porous scaffolds, Mater. Sci. Eng. C 32 (2012) 961–968, https://doi.org/10.1016/j.msec.2012.02.021.
[20] E. Weidner, Impregnation via supercritical CO_2 – What we know and what we need to know, J. Supercrit. Fluids 134 (2018) 220–227, https://doi.org/10.1016/j.supflu.2017.12.024.
[21] D. Stojanovic, A. Orlovic, S.B. Glisic, S. Markovic, V. Radmilovic, P.S. Uskokovic, R. Aleksic, Preparation of MEMO silane-coated SiO2 nanoparticles under high pressure of carbon dioxide and ethanol, J. Supercrit. Fluids 52 (2010) 276–284, https://doi.org/10.1016/j.supflu.2010.02.004.
[22] V.G. Correia, A.M. Ferraria, M.G. Pinho, A. Aguiar-Ricardo, Antimicrobial contact-active oligo(2-oxazoline)s-grafted surfaces for fast water disinfection at the point-of-use, Biomacromolecules 16 (2015) 3904–3915, https://doi.org/10.1021/acs.biomac.5b01243.
[23] W.Z. Xu, L. Yang, P.A. Charpentier, Preparation of antibacterial softwood via chemical attachment of quaternary ammonium compounds using supercritical CO_2, ACS Sustain. Chem. Eng. 4 (2016) 1551–1561, https://doi.org/10.1021/acssuschemeng.5b01488.
[24] C. Darpentigny, C. Sillard, M. Menneteau, E. Martinez, P.R. Marcoux, J. Bras, B. Jean, G. Nonglaton, Antibacterial cellulose nanopapers via aminosilane grafting in supercritical carbon dioxide, ACS Appl. Bio Mater. 3 (2020) 8402–8413, https://doi.org/10.1021/acsabm.0c00688.
[25] M. Tyrka, M. Nowak, D. Misic, T. Półbrat, S. Koter, A. Trusek, I. Zizovic, Cellulose acetate membranes modification by aminosilane grafting in supercritical carbon dioxide towards antibiofilm properties, Membranes 12 (2021) 33, https://doi.org/10.3390/membranes12010033.
[26] M.B. Yagci, S. Bolca, J.P.A. Heuts, W. Ming, G. de With, Self-stratifying antimicrobial polyurethane coatings, Prog. Org. Coat. 72 (2011) 305–314, https://doi.org/10.1016/j.porgcoat.2011.04.021.
[27] E.A. Saverina, N.A. Frolov, O.A. Kamanina, V.A. Arlyapov, A.N. Vereshchagin, V. P. Ananikov, From antibacterial to antibiofilm targeting: an emerging paradigm shift in the development of quaternary ammonium compounds (QACs), ACS Infect. Dis. 9 (2023) 394–422, https://doi.org/10.1021/acsinfecdis.2c00469.
[28] M. Nowak, D. Semba, D. Misic, T. Półbrat, D. Stojanovic, A. Trusek, I. Zizovic, Cellulose Acetate Modification Towards Antibiofilm Properties via Chemical Attachment of Quaternary Ammonium Compounds using Supercritical CO2, in: Montreal, 2022. ⟨https://supercriticalfluidsociety.net/issf-2022-montreal/⟩.
[29] Y. Zhou, Y. Jiang, Y. Zhang, L. Tan, Improvement of antibacterial and antifouling properties of a cellulose acetate membrane by surface grafting quaternary ammonium salt, ACS Appl. Mater. Interfaces 14 (2022) 38358–38369, https://doi.org/10.1021/acsami.2c09963.
[30] S. Milovanovic, D. Markovic, K. Aksentijevic, D.B. Stojanovic, J. Ivanovic, I. Zizovic, Application of cellulose acetate for controlled release of thymol, Carbohydr. Polym. 147 (2016) 344–353, https://doi.org/10.1016/j.carbpol.2016.03.093.

[31] D.A. Cerqueira, G. Rodrigues Filho, R.M.N. Assunção, A new value for the heat of fusion of a perfect crystal of cellulose acetate, Polym. Bull. 56 (2006) 475–484, https://doi.org/10.1007/s00289-006-0511-9.
[32] M. Sousa, A.R. Brás, H.I.M. Veiga, F.C. Ferreira, M.N. de Pinho, N.T. Correia, M. Dionísio, Dynamical characterization of a cellulose acetate polysaccharide, J. Phys. Chem. B. 114 (2010) 10939–10953, https://doi.org/10.1021/jp101665h.
[33] ISO 7218; Microbiology of Food and Animal Feeding Stuffs—General Rules for Microbiological Examinations, AMENDMENT 1, ISO 7218:1996/Amd.1:2001(E), Geneva, Switzerland, 2001., (n.d.).
[34] C.S.K. Achoundong, N. Bhuwania, S.K. Burgess, O. Karvan, J.R. Johnson, W. J. Koros, Silane modification of cellulose acetate dense films as materials for acid gas removal, Macromolecules 46 (2013) 5584–5594, https://doi.org/10.1021/ma4010583.
[35] A. Khalf, K. Singarapu, S.V. Madihally, Cellulose acetate core–shell structured electrospun fiber: fabrication and characterization, Cellulose 22 (2015) 1389–1400, https://doi.org/10.1007/s10570-015-0555-9.
[36] P.F. Andrade, A.F. de Faria, F.J. Quites, S.R. Oliveira, O.L. Alves, M.A.Z. Arruda, M. do C. Gonçalves, Inhibition of bacterial adhesion on cellulose acetate membranes containing silver nanoparticles, Cellulose 22 (2015) 3895–3906, https://doi.org/10.1007/s10570-015-0752-6.
[37] H. Kamal, F.M. Abd-Elrahim, S. Lotfy, Characterization and some properties of cellulose acetate-co-polyethylene oxide blends prepared by the use of gamma irradiation, J. Radiat. Res. Appl. Sci. 7 (2014) 146–153, https://doi.org/10.1016/j.jrras.2014.01.003.
[38] S. Waheed, A. Ahmad, S.M. Khan, S.- Gul, T. Jamil, A. Islam, T. Hussain, Synthesis, characterization, permeation and antibacterial properties of cellulose acetate/polyethylene glycol membranes modified with chitosan, Desalination 351 (2014) 59–69, https://doi.org/10.1016/j.desal.2014.07.019.
[39] T. Calvo-Correas, M.D. Martin, A. Retegi, N. Gabilondo, M.A. Corcuera, A. Eceiza, Synthesis and characterization of polyurethanes with high renewable carbon content and tailored properties, ACS Sustain. Chem. Eng. 4 (2016) 5684–5692, https://doi.org/10.1021/acssuschemeng.6b01578.
[40] A. Tenorio-Alfonso, M.C. Sánchez, J.M. Franco, Preparation, characterization and mechanical properties of bio-based polyurethane adhesives from isocyanate-functionalized cellulose acetate and castor oil for bonding wood, Polymers 9 (2017) 132, https://doi.org/10.3390/polym9040132.
[41] B.H. Stuart, Infrared spectroscopy: fundamentals and applications, 2009.
[42] M. Schilling, M. Bouchard, H. Khanjian, T. Learner, A. Phenix, R. Rivenc, Application of chemical and thermal analysis methods for studying cellulose ester plastics, Acc. Chem. Res. 43 (2010) 888–896, https://doi.org/10.1021/ar1000132.
[43] M. Kamimura, T. Kitazawa, Y. Yoshino, K. Tatsuno, K. Koike, Bacillus cereus as a pathogen and retention of medical devices are risk factors for Bacillus bacteremia, Int. J. Infect. Dis. 14 (2010), e391, https://doi.org/10.1016/j.ijid.2010.02.489.
[44] S. Galié, C. García-Gutiérrez, E.M. Miguélez, C.J. Villar, F. Lombó, Biofilms in the food industry: health aspects and control methods, Front. Microbiol. 9 (2018), 898, https://doi.org/10.3389/fmicb.2018.00898.
[45] R. Bland, J. Waite-Cusic, A.J. Weisberg, E.R. Riutta, J.H. Chang, J. Kovacevic, Adaptation to a commercial quaternary ammonium compound sanitizer leads to cross-resistance to select antibiotics in listeria monocytogenes isolated from fresh produce environments, Front. Microbiol. 12 (2022), 782920, https://doi.org/10.3389/fmicb.2021.782920.
[46] Y.-H. Hsueh, E.B. Somers, D. Lereclus, A.C.L. Wong, Biofilm formation by *Bacillus cereus* is influenced by PlcR, a pleiotropic regulator, Appl. Environ. Microbiol. 72 (2006) 5089–5092, https://doi.org/10.1128/AEM.00573-06.
[47] Y. Zheng, L. He, T.K. Asiamah, M. Otto, Colonization of medical devices by staphylococci: colonization of medical devices by staphylococci, Environ. Microbiol. 20 (2018) 3141–3153, https://doi.org/10.1111/1462-2920.14129.
[48] H.D. Isenberg, Molecular biology: molecular methods for antimicrobial agent resistance determination, in: H.D. Isenberg (Ed.), Clinical Microbiology Procedures Handbook, Vol. 2, American Society for Microbiology Press, Washington DC, USA., 2004.
[49] J. Gao, E.M. White, Q. Liu, J. Locklin, Evidence for the phospholipid sponge effect as the biocidal mechanism in surface-bound polyquaternary ammonium coatings with variable cross-linking density, ACS Appl. Mater. Interfaces 9 (2017) 7745–7751, https://doi.org/10.1021/acsami.6b14940.
[50] K. Lewis, A.M. Klibanov, Surpassing nature: rational design of sterile-surface materials, Trends Biotechnol. 23 (2005) 343–348, https://doi.org/10.1016/j.tibtech.2005.05.004.
[51] C. Andersen, J. Madsen, A.E. Daugaard, A synthetic overview of preparation protocols of nonmetallic, contact-active antimicrobial quaternary surfaces on polymer substrates, Macromol. Rapid Commun. 42 (2021), 2100437, https://doi.org/10.1002/marc.202100437.
[52] T. Gundolf, B. Rauch, R. Kalb, P. Rossmanith, P. Mester, Influence of bacterial lipopolysaccharide modifications on the efficacy of antimicrobial ionic liquids, J. Mol. Liq. 271 (2018) 220–227, https://doi.org/10.1016/j.molliq.2018.08.134.
[53] A. Casadevall, F.C. Fang, Reproducible science, Infect. Immun. 78 (2010) 4972–4975, https://doi.org/10.1128/IAI.00908-10.
[54] S. Kreve, A.C.D. Reis, Bacterial adhesion to biomaterials: What regulates this attachment? A review, Jpn. Dent. Sci. Rev. 57 (2021) 85–96, https://doi.org/10.1016/j.jdsr.2021.05.003.
[55] Laboratory of Biomechanics and Biomedical Engineering, Department of Mechanical Engineering, University of Patras, Patras, Greece, M. Katsikogianni, Y. Missirlis, Concise review of mechanisms of bacterial adhesion to biomaterials and of techniques used in estimating bacteria-material interactions, Eur. Cell. Mater. 8 (2004) 37–57. https://doi.org/10.22203/eCM.v008a05.
[56] S. Milovanovic, T. Adamovic, K. Aksentijevic, D. Misic, J. Ivanovic, I. Zizovic, Cellulose acetate based material with antibacterial properties created by supercritical solvent impregnation, Int. J. Polym. Sci. 2017 (2017) 1–9, https://doi.org/10.1155/2017/8762649.
[57] I. Zizovic, L. Senerovic, I. Moric, T. Adamovic, M. Jovanovic, M.K. Krusic, D. Misic, D. Stojanovic, S. Milovanovic, Utilization of supercritical carbon dioxide in fabrication of cellulose acetate films with anti-biofilm effects against Pseudomonas aeruginosa and Staphylococcus aureus, J. Supercrit. Fluids 140 (2018) 11–20, https://doi.org/10.1016/j.supflu.2018.05.025.
[58] ASTM Standards, ASTM E2149–20 Standard Test Method for Determining the Antimicrobial Activity of Antimicrobial Agents Under Dynamic Contact Conditions, (2020). ⟨https://www.astm.org/e2149–20.html⟩.
[59] A. Rojas, A. Torres, A. Añazco, C. Villegas, M.J. Galotto, A. Guarda, J. Romero, Effect of pressure and time on scCO2-assisted incorporation of thymol into LDPE-based nanocomposites for active food packaging, J. CO_2 Util. 26 (2018) 434–444, https://doi.org/10.1016/j.jcou.2018.05.031.
[60] NATEX Prozesstechnologie, High Pressure Quick Acting Closure System for Wood Impregnation, ⟨https://www.natex.at/fileadmin/content/PDFs/closure_system_wood_impregnation.pdf⟩ (accessed August 11, 2023).
[61] DyeCo, CO2 dyeing, ⟨https://dyecoo.com/⟩ (accessed August 11, 2023).
[62] A. Barros, Hydrumedical – Supercritical fluid technologies in medical devices, from impregnation to sterilization, In: Proceedings of the First Greenering International Conference, Costa da Caparica, Portugal (Virtual event), 2021, Kaynote Lect.,. Book of Abstracts pg. 14. ⟨https://www.greenering.eu/images/greenering/documents/1st_conference_book_of_abstracts.pdf⟩.
[63] E. Rój, ed., Supercritical fluid applications: supercritical fluids - the current state and outlook, New Chemical Syntheses Institute, Puławy, 2016. ISBN 978–83-935354–1-5.
[64] D.F. Tirado, A. Cabañas, L. Calvo, Modelling and scaling-up of a supercritical fluid extraction of emulsions process, Processes 11 (2023) 1063, https://doi.org/10.3390/pr11041063.
[65] C. Wolf, J. Maninger, K. Lederer, H. Frühwirth-Smounig, T. Gamse, R. Marr, Stabilisation of crosslinked ultra-high molecular weight polyethylene (UHMW-PE)-acetabular components with α-tocopherol, J. Mater. Sci. Mater. Med. 17 (2006) 1323–1331, https://doi.org/10.1007/s10856-006-0607-7.
[66] T. Gamse, R. Marr, C. Wolf, K. Lederer, Supercritical CO_2 impregnation of polyethylene components for medical purposes, Hem. Ind. 61 (2007) 229–232, https://doi.org/10.2298/HEMIND0704229G.
[67] I. Zizovic, M. Tyrka, K. Matyja, I. Moric, L. Senerovic, A. Trusek, Functional modification of cellulose acetate microfiltration membranes by supercritical solvent impregnation, Molecules 26 (2021) 411, https://doi.org/10.3390/molecules26020411.
[68] I. Zizovic, A. Trusek, M. Tyrka, I. Moric, L. Senerovic, Functionalization of polyamide microfiltration membranes by supercritical solvent impregnation, J. Supercrit. Fluids 174 (2021), 105250, https://doi.org/10.1016/j.supflu.2021.105250.